

# The influence of the Arctic on European weather and climate

---

Master Thesis in Postgraduated Environmental  
Physics (PEP)

**Marta Anna Kasper**

**16.08.2013**

**Universität Bremen**

**Alfred-Wegener-Institut Helmholtz-Zentrum für Polar- und  
Meeresforschung**

Supervised by:

Prof. Dr. Thomas Jung

Dr. Martin Werner



## Acknowledgements

Firstly I want to thank Prof. Dr. Thomas Jung for accepting me in his research group and providing me with such an exciting topic. Exploring the impact of the Arctic on Europe was definitely a great adventure even though the Thesis was completely based on computer simulations.

I want to thank Prof. Jung, Dr. Martin Werner and Dr. Tido Semmler for all their support and help during the work. I'm really grateful for their time, all discussions, explanations, hints and ideas. Furthermore, I thank Prof. Jung and Dr. Werner for the supervision of this Thesis.

I also owe thanks to Dr. Suomia Serrar for providing the experiment data and Matlab code for reading the data, as well as for her advice and support while analyzing the data.

Furthermore, I thank the colleagues from Climate Dynamic group, especially Helge Goessling, Stephan Juricke and Thomas Rackow for all discussions, hints and ideas that improved this Thesis.

Finally I thank my family who enabled me to pursue a study and life in Germany and let me go my own way.

## Abstract

Polar Regions are key components in the development of the global circulation system and therefore the impact of Arctic on European climate is beyond doubt. Moreover, recent studies show that the sea ice is playing bigger role than it has been assumed before, e.g. there seems to be negative correlation between sea ice concentration and strength of high pressure system over Siberia in winter (*Wu et al, 2011*). In addition, due to the warming of the climate, the Arctic is changing more than any other region on Earth. On the other hand, extended-range (11-30 days) weather forecasts are of high interest but are still not very accurate.

To investigate whether the error of the extended-range weather forecasts could origin in the Arctic, numerical experiments applying relaxation technique, also called nudging were done. Prognostic variables of the atmospheric component of the ECMWF Integrated Forecasting System (IFS) were corrected by re-analysis data (ERA40 and ERA-Interim) reducing the error of the forecast in the relaxation region.

Applying the relaxation technique to the Arctic shows that the better knowledge of this region indeed improves the quality of the weather forecast for Europe therefore there must be a link between the Arctic and Europe. However, the strength of the impact depends on the season, area of relaxation and investigated region. The strongest improvement could be observed for northern and eastern Europe in winter and spring if the relaxation was applied to the area north of 70°N.

Furthermore it was shown, that the improvement of the forecast quality due to relaxation could be linked to an anomalous northerly wind transporting cold air masses across Scandinavia towards Europe, especially in winter.

In addition, in winter months the impact of the Arctic for almost whole Europe was higher than that of the Tropics.

The outcome of the study shows that the impact of the Arctic on European weather and climate is significant and it would be beneficial to have better observing system in that region. Furthermore, it proves that the relaxation technique is a powerful tool to search for origin of the forecasts error as well to investigate remote impacts of a defined region.

<b>ACKNOWLEDGEMENTS</b>	<b>3</b>
<b>ABSTRACT</b>	<b>4</b>
<b>1 INTRODUCTION</b>	<b>6</b>
<b>2 BACKGROUND ON WEATHER FORECASTING</b>	<b>9</b>
2.1 WEATHER FORECASTING	9
2.2 FORECAST ERROR	10
2.3 RELAXATION METHOD	11
2.4 GEOPOTENTIAL HEIGHT	13
<b>3 METHODOLOGY</b>	<b>14</b>
3.1 MODEL AND DATA	14
3.2 RELAXATION EXPERIMENT	14
3.3 ANALYSIS OF THE DATA: MEAN IMPACT	16
3.4 ANALYSIS OF THE DATA: FLOW DEPENDENCE	18
<b>4 RESULTS</b>	<b>21</b>
4.1 WINTER-ONLY MONTHLY FORECASTS	21
4.2 ALL-SEASONS MEDIUM RANGE FORECASTS	35
<b>5 SUMMARY AND DISCUSSION</b>	<b>47</b>
<b>6 CONCLUSIONS AND OUTLOOK</b>	<b>51</b>
<b>7 REFERENCES</b>	<b>53</b>
<b>8 APPENDIX</b>	<b>55</b>
<b>9 LIST OF FIGURES</b>	<b>61</b>

# 1 Introduction

Predicting weather is an important and valuable skill. Apart from answering obvious questions such as “Do I need an umbrella tomorrow?” knowing weather in advance can be much more important. One example is extreme weather events like hurricanes, droughts, or heavy storms. If these could be predicted well enough in advance, some protective measures could be taken e.g. people from areas at risk could be evacuated. Accurate forecasts of storms and winds are crucial for ships and planes in order to choose the safest and cheapest route. Furthermore seasonal weather forecast can be important for the industry e.g. if very cold winter is expected, fuel prices can be adjusted.

In the recent decades the quality of the produced forecasts improved tremendously and nowadays useful predictions can be made on average 8 days ahead, but the error for longer time ranges (beyond day 15) is high (*Simmons and Hollingsworth, 2001, Richardson et al., 2009*). As the atmosphere is very complex and some processes and teleconnections are still unknown, it could be beneficial to look if there are certain regions where the forecast error originates. Modern numerical weather prediction (NWP) systems consisting of sophisticated numerical models, high efficiency supercomputers and advanced observing systems provide a very good opportunity for such investigations. If the forecast error made in some region could be artificially reduced, the importance and remote impact of this region could be tested.

Generally, the European weather is influenced by the interplay between two circulation cells: the Polar Cell and the Ferrel Cell. Close to the surface warm air masses from the tropics and subtropics flowing northwards and cold air masses from the poles flowing southwards collide. As a consequence baroclinic instabilities develop leading to the formation of eddies (cyclones and anticyclones) that determine the daily variability of the weather.

Europe can be divided in three climatic zones: subtropical climate in the Mediterranean region, typical mid-latitudes climate in central Europe, and subpolar climate in northern Europe. In this Thesis the focus will be on central and northern Europe, as for these regions the impact of the Arctic is stronger.

Weather in Europe is strongly influenced by the westerly mean flow; however, locally the main wind direction can be different. Furthermore, the climate in Europe can be divided into maritime and continental. In Western Europe, especially in coastal

regions, the climate is strongly influenced by oceanic air masses that are moist and relatively warm (cold) in the winter (summer) while, Eastern Europe is more often influenced by continental air masses that are dry and cold (hot) in winter (summer) (*Berry and Chorley, 2010*).

It is also known, that persistent large-scale circulation anomalies like the North Atlantic Oscillation (NAO) and the closely related Arctic Oscillation (AO) have an impact on the European weather, determining the main direction of the air flow, especially during winter (*Berry and Chorley, 2010*). While the NAO is negative, easterlies are stronger, bringing cold air from Siberia towards Europe. Also while AO is negative colder winters are expected in Europe as the polar vortex is weaker and polar air masses are transported further south with north-easterly winds.

Various studies show that the role of the Arctic has been underestimated as the sea ice seems to be an important component. *Wu et al (2011)* found that there is a negative correlation between the sea ice concentration in the Arctic (especially in Eastern Arctic Ocean and on Siberian coasts) during autumn and winter and the strength of the Siberian High in winter. With decrease of sea ice concentration, the Siberian High will be stronger, leading to colder winters in Europe, especially during the negative phase of NAO. In this study it was also shown that the winter Siberian High cannot be predicted using only tropical sea surface temperature, but the knowledge of Arctic sea ice concentration is necessary (*Wu et al. 2011*). Furthermore *Jaiser et al.(2011)* investigated the impact of the sea ice on the development of baroclinic instabilities, and found that through reduced sea ice concentration in autumn baroclinic instabilities onset earlier and this influences also large-scale planetary waves in the following winter.

In another study *Semmler et al.(2012)* investigated in idealized experiments the influence of reduced and absent sea ice in the Arctic on the energy budget and climate of the Northern Hemisphere. Under such conditions the Arctic absorbs more shortwave radiation in summer and, due to increased temperature, emits more longwave radiation in following winter, with a net energy gain. The meridional temperature gradient between equator and the Arctic decreases and the circulation cells are weaker. Other consequences are increased latent heat flux and resulting increased precipitation in the Arctic in winter, but decreased precipitation in the adjacent regions. After considering various possible effects, *Semmler et al* predict

that, through the reduction of sea ice, less extreme cold events can be expected for the mid – latitudes in a warmer future climate.

There is clearly some evidence for the impact of the Arctic on mid-latitudes; however, the links from the tropics are better understood (e.g. El Nino Southern Oscillation) (*Berry and Chorley, 2010*). In addition, due to the warming of the climate, the Arctic is changing more rapidly than any other region on Earth. The presence of the cryosphere and its interplay with the ocean determines the climate there. The two components have very different properties: on the one hand, ice (and snow) reflects most of the solar radiation (high albedo) and the ocean absorbs most of the solar radiation (low albedo). As the air temperature rises and ice melts the area of the ocean increases. Therefore more solar energy is absorbed by the ocean and this leads to further warming of water and increased sea ice melting. This positive feedback mechanism is known as ice-albedo feedback. On the other hand, ice is a good isolator, preventing the heat exchange between the ocean and the atmosphere. If the sea ice melts, the atmosphere will be additionally warmed by the ocean (*Lemke et al., 2007*). Therefore it is highly interesting to investigate the connection between Europe and the Arctic and eventually find out how these new conditions in the Arctic will influence the European weather and climate.

The Thesis is based on numerical experiments that have previously been performed using an operational weather forecasting system. To understand the remote impact of the Arctic (and the Tropics) on European weather, in these experiments the error of the forecast in the Arctic was artificially reduced by applying relaxation technique that is also known as nudging. In each time step of the integration the model state was corrected (relaxed) towards observational data. This method has been successfully used in the past for similar studies (*Jung et al. 2010a, 2010b, 2011, Klinker 1990*) and seems suitable for such investigations, especially because the quality and quantity of the data is improving.

The objective of this Thesis is to analyze and evaluate the described experimental data. The first aim is to investigate whether the quality of weather forecasts for Europe could be improved with a better knowledge of the Arctic (i.e. better forecasts). If this is the case, it can be concluded that the Arctic indeed has a significant impact on European weather. The second aim of the Thesis is to examine if the (expected) impact of the Arctic can be linked to certain atmospheric circulation patterns, how



these links depend on the season and, eventually, what role the warming of the climate plays.

In the next chapters some background information on weather forecasting as well as the used model and data is presented. This is followed by a detailed description of the relaxation formulation and the methods used to analyze the data obtained from the experiments. Thereafter the results are presented, starting with a set of experiment for boreal winter, followed by more comprehensive set of experiments set for all seasons. Finally the results are discussed and summarized.

## 2 Background on weather forecasting

### 2.1 Weather forecasting

In the past, predicting the weather for the next days was based on observation of current state of the atmosphere and knowledge about previous states (*empirical forecast*). Forecasters that were trained for that purpose knew that certain phenomena are usually followed by other phenomena e.g. that cirrus clouds are indicating warm and nice weather (as the warm front is passing). In 1904 Vilhelm Bjerknes realized that physical laws can be used to predict weather (*Lynch, 2007*). He proposed that, knowing the current state of the atmosphere and the equations governing the motion in the atmosphere, future states can be calculated (*deterministic forecast*). Furthermore he listed seven basic variables that should describe the state of the atmosphere (three components of the velocity, pressure, temperature, air density and humidity) as well as seven equations and proposed a graphical method for solving them. However, at that time it was impossible to apply this method, as there were not enough observations.

The idea was further tested during the First World War by Lewis Fry Richardson, who computed a forecast using essentially Bjerknes' approach. Unfortunately, the results were very unrealistic due to lacking knowledge of processes in the atmosphere and numerical techniques. Furthermore, it took months to produce a 6-hour forecast which made the method completely useless at that time. Only the invention of computers in the 1940s made numerical forecast feasible and it they became a real alternative to the empirical forecasts.

Nowadays numerical weather prediction (NWP) is widely used as the by far best way to produce accurate forecasts. Modern high efficiency computers make it possible not only to calculate single forecasts with high temporal and spatial resolution, but also to produce ensembles of forecasts. Such an ensemble consists of many single forecasts, each with slightly perturbed initial conditions, allowing for a statement about the probability distribution of the obtained result (*ensemble forecast*). Current operational systems are capable to complete the forecast cycle, including collecting of observational data, calculating the forecast and distributing the information to the public, within 6 hours. In the slightly more than 100 years since Bjerknes presented his idea, the development of the components of the prediction system was huge.

## 2.2 Forecast error

One measure that is often used to describe the skill of a forecast is the anomaly correlation coefficient (ACC) of the 500 hPa geopotential height of the forecast field with respect to the observed state. If the ACC is above 60%, the forecast is considered useful. Modern forecast systems drop below the 60% limit on average on day 8, which means that the 500hPa geopotential height field can be predicted with 60% correlation on average up to 8 days ahead. Therefore after day 8 the forecast has too big error and is considered useless (*Richardson, 2009*).

In **Figure 1** an example of a weather forecast of geopotential height at 500hPa for the grid point at 77.5°N and 45°E (black curve) is shown together with corresponding observations (blue curve). The forecast is performing very well in the first five days, but then the forecast starts to differ more and more from the observations. However, between day 10 and day 14 the forecast is again pretty well. Beyond day 18 the forecast and observations curves diverge and the forecast becomes completely useless as it is not able to reproduce the increase of the geopotential height. Comparing to the mean value of day 8, this example shows a relatively good forecast. Furthermore two statements may be inferred from this example: first, the forecast error grows with the time of the forecast, and second, good agreement of the forecast and data can be achieved by chance (day 10-day 14).

The growth of the forecast error has many reasons. The atmosphere is very complex: it includes many processes on different temporal and spatial scales, ranging (from planetary waves to the microstructure of clouds, that all need to be considered in the

model. The continuous equations must be discretized onto a finite number of grid points to allow for their integration, where the choice of the temporal and spatial resolution is crucial to the quality of a forecast. On the one hand, the resolution is limited by the available computational power, on the other hand by the scale of the processes. Furthermore the initial conditions necessary to start a forecast are not perfectly known. Through parameterization of subscale processes, simplifications in the model as well as interpolation and averaging (both of initial conditions and results), the outcome of a model will never represent the true state of the atmosphere. As each state is calculated from a previous state, the error will increase in time. And most importantly, the atmosphere has a chaotic nature, which means that already very small changes in the initial conditions inevitably lead to completely different results of the forecast after some time (*Lorenz, 1963*). Due to the nonlinearities in the equations, any perturbation of the initial conditions will grow. Therefore the error of a forecast cannot be avoided completely, but only reduced.

### 2.3 Relaxation method

Newtonian relaxation, also called nudging, is one of the simplest methods for incorporating observational data into models (*data assimilation*) (*Kalnay, 2003*). At each time step of the integration model state is drawn towards some reference data. If the reference data are observational data, the model state is kept close to reality (error of the forecast is reduced).

Relaxation is realized by adding to the prognostic equation an extra term of the form

$$-\lambda(\mathbf{x} - \mathbf{x}^{\text{ref}}) \quad (1)$$

where  $\mathbf{x}$  is the prognostic variable,  $\mathbf{x}^{\text{ref}}$  is the value towards which the model state is drawn, and  $\lambda$  is relaxation the strength parameter defined as:

$$\lambda = \frac{\text{strength of relaxation}}{\text{time step}} \quad (2)$$

The following example shows the relaxation of the zonal velocity  $u$  :

$$\frac{\partial u}{\partial t} = -u \frac{\partial u}{\partial x} - v \frac{\partial u}{\partial y} + fv - \frac{\partial \phi}{\partial x} - \lambda(u - u^{\text{ref}}) \quad (3)$$

Where  $t$  is time,  $x$  and  $y$  are the zonal and meridional coordinates, respectively,  $u$  and  $v$  zonal and meridional velocities, respectively,  $\phi$  the latitude,  $f$  the Coriolis frequency.

Setting  $\lambda = 0.1/\Delta t$  means that the relaxed zonal velocity  $u$  is calculated in each time step by subtracting from the primary resulting zonal velocity  $u$  10% of the difference between it and the corresponding value in the reference data.

In **Figure 1** an example of a relaxation is shown (red dashed curve). Applying the relaxation in each time step strongly reduces the forecast error and the result is very close to the reference data. In the shown example the relaxation is especially efficient after day 20. Although the relaxed forecast still differs from the observations, it is able to reproduce the trend.

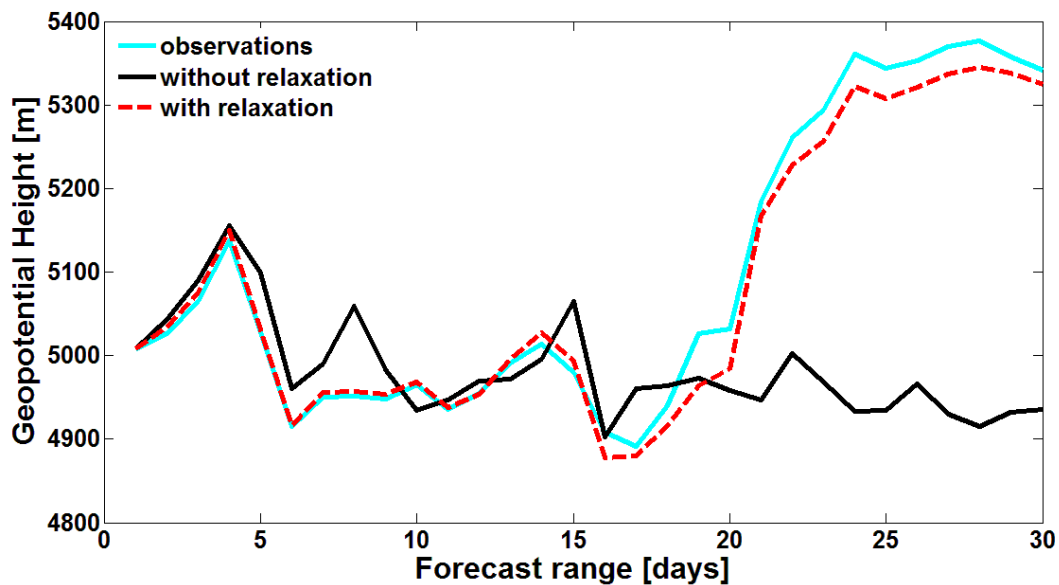


**Figure 1** An example of a 30-day forecast (black), relaxed forecast (dashed, red) and corresponding observations (blue). The parameter is the geopotential height at 500 hPa level, for the grid point 77.5°N and 45°E, the forecast started on 15<sup>th</sup> February 1982.

## 2.4 Geopotential height

The geopotential  $\Phi(z)$  is the amount of work that is needed to lift a mass of one kilogram from the sea level to a height  $z$  (by convention the geopotential at sea level is zero):

$$\Phi(z) = \int_0^z d\Phi = \int_0^z g dz \quad (4)$$

Where  $g$  is the apparent gravity. Furthermore, the geopotential is another way to express pressure  $p$  and density  $\rho$  of an air layer, as assuming hydrostatic balance the geopotential is defined as:

$$\frac{dp}{dz} = -\rho g \quad (5)$$

$$g dz = d\Phi = -\frac{dp}{\rho} \quad (6)$$

Therefore is very often used for meteorological applications as the equations governing the motion in the atmosphere can be much easier calculated in terms of geopotential than pressure and density.

The geopotential height  $Z$  is the geopotential  $\Phi(z)$  divided by the globally averaged acceleration due to gravity at the sea level  $g_0 = 9.80665 \text{ ms}^{-2}$

$$Z = \frac{\Phi(z)}{g_0} \quad (7)$$

Usually the geopotential height  $Z$  is given at a specific pressure level, indicating at which height the pressure level can be found at that location. The geopotential height of the 500hPa level (hereafter Z500) is a widely used parameter to describe the atmospheric flow in the middle and upper troposphere, whereby high geopotential height  $Z$  reflects high pressure (*Holton, 2004*).

## 3 Methodology

### 3.1 Model and data

The numerical experiments analyzed in this Thesis were conducted using the operational weather forecast model of the European Centre for Medium-Range Weather Forecasts (ECMWF), one of the world's leading centers for NWP. The Integrated Forecast System (IFS) is a comprehensive and complex atmosphere model that can produce deterministic forecasts as well as ensemble forecasts. The wide range of implemented dynamical and physical processes, state-of-the-art numerical techniques, advanced data assimilation techniques as well as high quality observational data make it one of the world's best NWP models for predicting synoptic-scale processes on the medium range.

The data used for the experiments was taken from the ECMWF re-analysis. This dataset was produced using data from all available observation platforms (satellites, ground-based stations, radiosondes, balloons, moorings) from the past and present and combining these with short range model simulations. The model simulations are produced with a "frozen NWP", meaning that the same version of the model is used for all simulations. This technique reduces the error of the model and the observations, making the re-analysis a good estimate of past atmospheric states. In the experiments two re-analyses were used: ERA-40 (covering the years from 1957 to 2002) and ERA-Interim (covering the years from 1979 to present) (*Uppala et al. 2005, Dee et al. 2011*).

### 3.2 Relaxation Experiment

The general idea behind the experiments is to use an operational weather forecast model and data from the past to calculate (re-)forecasts to investigate the influence of the Arctic on European weather. In first step a "normal" forecast is produced. In second step a new forecast, applying the relaxation technique to artificially reduce the error in a pre-defined region, is produced. Finally both forecasts can be compared.

In this Thesis data from experiments with two different settings were analyzed. The purpose of the first set of experiments is to determine if an influence of the Arctic on European weather can be found during boreal winter when the impact of the Arctic is

expected to be strongest and how strong is this influence compared to that of the tropics. A relatively small data set was produced that contains 88 monthly (30 days) weather forecasts from 1980 to 2002(see 3.2.1). In the second set of experiments the analysis is extended over the all months from 1979 to 2012. Furthermore the forecasts were produced with higher temporal and spatial resolution, but due to limited computational power, the forecast range was reduced to 14 days. Nevertheless, a much bigger sample (204 forecasts for each season) was created that should increase the statistical significance and hence decrease the uncertainty of the result (see 3.2.2).

### 3.2.1 Winter-only monthly forecasts

As described in *Jung et al. (2010a)*, forecasts were generated with the model cycle 32r2 of IFS used at ECMWF from the 5th of June to the 5th of November 2007, with a spatial resolution of TL159 corresponding to  $1.125^\circ$  in the horizontal and 60 vertical levels. The forecasts were carried out for 30 days, with a time step of 1 hour, the data was used every 24 hours (0000UTC). The data from 22 years from 1980 to 2002 was used, producing 4 forecasts per year, each starting at the 15th of November, December, January and February, giving in total 88 forecast members. For all experiments sea surface temperature (SST) and sea ice fields were persisted during the forecast.

The relaxation was applied to zonal and meridional wind components, the temperature, and the logarithm of the surface pressure within a certain relaxation area. To smooth the border of the relaxation area, a hyperbolic tangent over a  $20^\circ$  wide zonal belt was applied. In this region  $\lambda$  increases smoothly from  $\lambda=0$  to a desired value, with the nominal border of the relaxation area in the middle of the  $20^\circ$  belt. Where not mentioned otherwise,  $\lambda$  is set to  $0.1/\Delta t$  (for more details see in *Jung et al, 2010a*).

The reference data were taken from ERA40, which is available at 6 hourly resolution (0000, 0600, 1200, 1800 UTC). At time steps where no direct data were available, linear interpolation was applied. The ERA40 data were used for the initial conditions as well as for the relaxation. This means, in each time step the relaxation was carried out using re-analysis data from exactly the same point in time and space.

For this Thesis four different forecast types were analyzed: the control runs (CNT) without relaxation and three corresponding runs with the atmosphere relaxed in the Arctic north of 70°N (R70), north of 80°N (R80) and in the tropics between 20°S and 20°N (TROP).

### 3.2.2 All-seasons medium range forecasts

The second set of forecasts was carried out with the model cycle 38r1 of IFS , which is operating at ECMWF since the 19<sup>th</sup> of June 2012, with a spatial resolution of TL255 corresponding to 0.7° in the horizontal and 60 vertical levels. All forecasts were carried out for 14 days with a time step of 1 hour, model results were used every six hours (0000, 0006,0012,0018 UTC).

Two forecasts were computed for each month between January 1979 and December 2012, the first one starting on the 1<sup>st</sup> day of the month and the second one starting on the 15<sup>th</sup> day of the month. To study the seasonality of the impact, the year was divided into four seasons: winter (December, January, February), spring (March, April, May), summer (June, July, August) and autumn (September, October, November). In total 204 forecast members were generated for each season. SST and sea ice fields were persisted through the forecast. The reference data was taken from the ERA-Interim re-analysis.

The relaxation was applied in the same way as for the winter only experiments, except that in the addition to the control run (CNT) only one corresponding relaxed forecast was produced. The atmosphere in the polar regions north of 75°N and south of 75°S was relaxed (R75) at the same time. As the time range of the forecast is short, there is not enough time for the signal from the well separated relaxation area in the South Hemisphere to propagate across the equatorial region. One can thus assume that in the considered time range of 14 days the relaxation over the Antarctic does not impact Europe.

### 3.3 Analysis of the data: mean impact

For the analysis of the monthly winter-only experiments, the data has been mapped to a 2.5° grid to decrease the computational effort. The variation of Z500 is still well captured at the chosen resolution. In the second step the 30-days data was averaged



over time window of 5 days to reduce the noise of the data (caused mainly by the passage of low pressure systems). Each 5-day mean is built of 5 members, i.e. for the first: day 1 to day 5, for the second: day 6 to day 10 and so on.

For the analysis of the all-seasons medium range forecasts the data was remapped to a 2.5° grid as well. Analogue to the first experiment, the data was averaged over time windows of 24 hours.

Finally the following steps (Sect. 3.3.1 to 3.4.2) were carried out for both sets of experiments.

### 3.3.1 Forecast error and mean forecast error

The forecast error ( $FE$ ) is the absolute difference between the model state and the re-analysis state. The mean forecast error ( $\overline{FE}$ ) is area-weighted spatial average of the forecast error, averaged over all forecast members (e.g. 88 for winter-only forecasts).

### 3.3.2 Error reduction

The error reduction  $ERed$  quantifies how much the forecast error is reduced by the relaxation compared to CNT.  $ERed$  is the difference between the  $FE$  of CNT and  $FE$  of the relaxed forecast, divided by the forecast error of CNT

$$ERed = \frac{FE(CNT) - FE(Relaxed)}{FE(CNT)} \times 100\% \quad (8)$$

For the mean error reduction the mean forecast error  $\overline{FE}$  averaged over some region was considered. For the spatially resolved plots of the error reduction averaged over forecast members was considered for each grid point separately.

### 3.3.3 Correlation

The correlation coefficient is a measure of linear dependence between two data samples. If the correlation coefficient is equal to 1 (-1), two data sets are perfect positive (negative) linear dependent.

In this study the correlation coefficient between the re-analysis data and forecast was calculated to investigate how well the forecast can reproduce the re-analysis (the higher the correlation coefficient, the better the forecast) .Correlation coefficients were calculated for each grid point and time window separately.

### 3.4 Analysis of the data: flow dependence

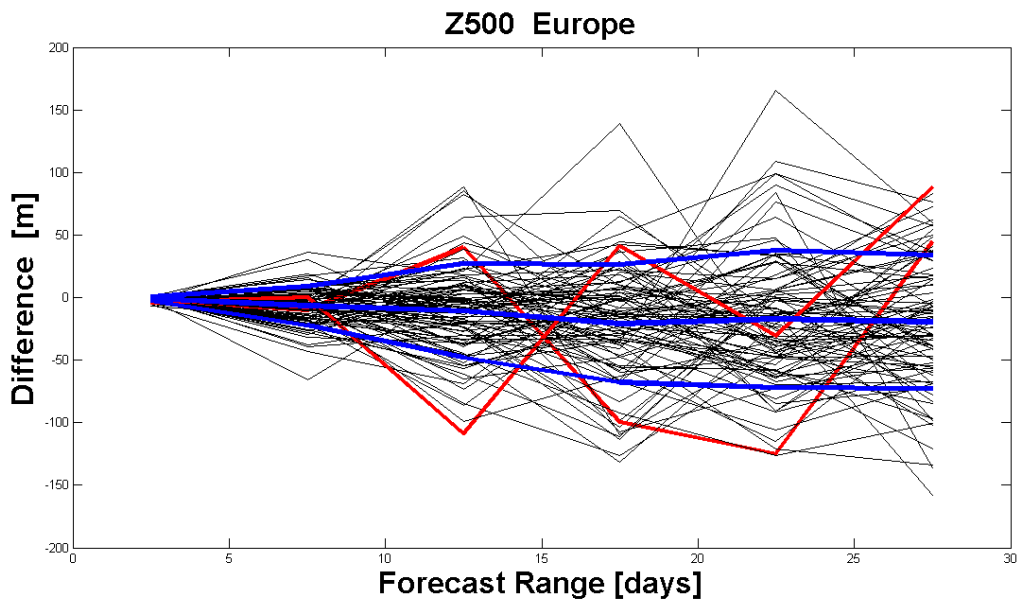


**Figure 2** The difference between forecast error (averaged over Europe) between CNT and forecast relaxed above 70°N of all 88 forecast members. Mean value and the limit of one standard deviation are shown with blue curves. Two examples are highlighted with red curves.

#### 3.4.1 Composite plots

To examine if the mean impact of the Arctic expressed by the mean forecast error ( $\overline{FE}$ ) and the error reduction ( $ERed$ ) is linked to specific atmospheric situations (*flow dependence*), composite analysis was performed. The idea is to choose forecast members that are exceptionally good or bad and examine the atmospheric conditions at which these forecast members were produced. The analysis can be summarized in the following four steps.

Step 1: The considered situation must be defined.

Here the goal of the analysis was to find out if there are situations when the relaxed forecasts are exceptionally better (or worse) than CNT (hence the forecast members will be “good” and “bad”, respectively). To this end the error of each forecast member

was averaged over Europe. Then the difference of the forecast error ( $FE$ ) between the relaxed forecasts and CNT, as well as the mean forecast error ( $\overline{FE}$ ) and its standard deviation were calculated (**Figure 2**).

Step 2: Forecast members that fulfill the requirement specified in Step 1 should be chosen from all forecast members.

If a forecast member exceeds the limit of the mean value plus (minus) the standard deviation, it is considered as “bad” (“good”). However, the variability within single forecast member is very high. Two examples are shown in **Figure 2** with red curves. One forecast member is rather “bad” for day 1 to day 15 as well as from day 26 to day 30, but “good” from day 16 to day 25. It was not possible to find forecast members that are above or below the limit during the whole forecast range (30 days). Considering only 15-days periods instead of the full 30 days was only slightly better, delivering in the first set of experiments approx. 4 forecast members each for both “good” and “bad” which is an insufficient sample size.

To improve the statistics, another approach was chosen, in which each 5-day window was considered separately. Then all single 5-day windows were grouped together over a time period of 15 days (all “good” from day1-day5, day6-day10 and day11-day15). The sizes of the samples that could be used for the composites applying this approach are shown in **Figure 3** for the first set of experiments and **Figure 4** for the second set of experiments. The sample size in the second set of experiments was considerably increased, e.g. in the first set of experiments for 5-day average for days 1-15 only 38 time-windows were “good”, while for the second set of experiments, for winter there were 306 “good” in for days 1-14.

Step 3: The atmospheric conditions for the forecast members chosen in Step 2 are considered.

For each of the 5-day window that was “good” (“bad”), the corresponding (the same forecast member, the same time window) atmospheric conditions (Z500 fields) were taken from re-analysis.

Step 4: The composites (means over all Z500 fields for “good” and “bad” forecast) were calculated, and finally the difference between them (“good”-“bad”) could be analyzed.

		"good"	"bad"
<b>5d average</b>	day 1-15	38	29
	day16-30	34	39
<b>3d average</b>	day 1-15	68	57
	day16-30	69	63

**Figure 3** It was looked for forecast members, for which the R70 was much better (“good”) or worse (“bad”) than CNT. Each time window was considered separately, to increase sample size, forecast members were grouped over larger time periods. The chart shows the sample sizes for the winter-only experiment, in dependence to chosen time period (day1-day15 or day16-day30) and time window chosen to average the data (3 or 5 days).

		"good"	"bad"
<b>Winter</b>	day1-7	190	138
	day8-14	216	202
<b>Spring</b>	day1-7	163	125
	day8-14	194	194
<b>Summer</b>	day1-7	173	159
	day8-14	192	191
<b>Autumn</b>	day1-7	169	165
	day8-14	202	184

**Figure 4** The same as in **Figure 3**, but for the all-seasons experiment.

### 3.4.2 Statistical significance of the composite differences

As already mentioned the variability within single forecast member and between different forecast members was high. Therefore it was not surprising that the variability within re-analysis fields for “good” (and “bad”) was high. To analyze the significance of the calculated difference, first the standard deviation of composites was calculated. Then the statistical significance of the difference was calculated with the Mann-Whitney U test (also called Wilcoxon rank-sum test). It is a non-parametric statistical test that can be used for investigating whether the means of two samples are significantly different. The data from the experiments was not distributed normally; therefore Student’s t-test was not applicable.

## 4 Results

### 4.1 Winter-only monthly forecasts

#### 4.1.1 Mean impact

To study the mean impact of the Arctic first the mean forecast error  $\overline{FE}$  was calculated for Northern Hemisphere Extratropics (NHE) between 40°N-90°N. As the relaxation region is within the investigated area is not surprising that the error of the forecast is reduced (shown in the Appendix). To better illustrate the impact of the relaxation on remote regions, two further investigation areas were defined: the mid-latitudes between 40°N (**Figure 5**, left) and 60°N and Europe between 40°N and 60°N and between 20°W and 40°E (**Figure 5**, right).

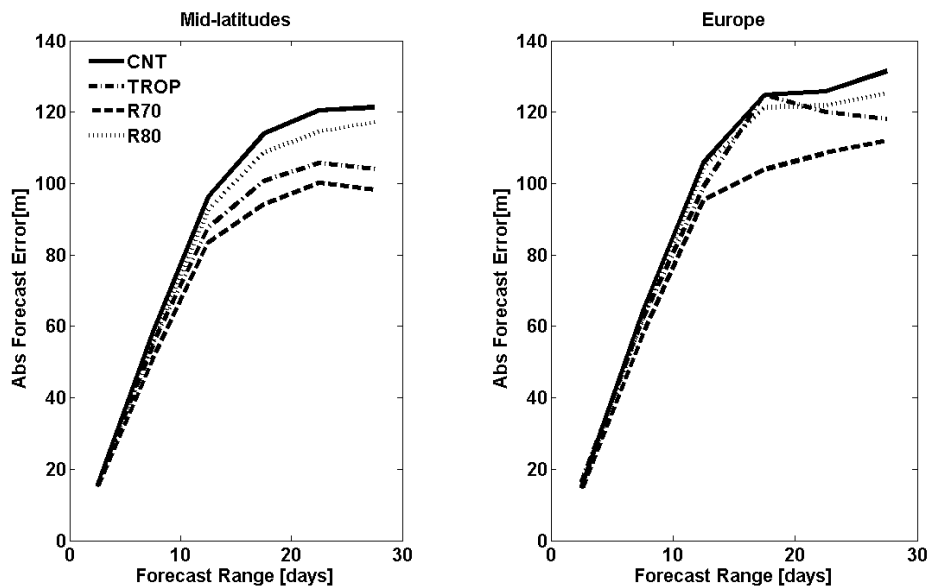


**Figure 5** Mean absolute error for 5-day-averaged forecasts of 500hPa geopotential height fields (m) over Mid-latitudes between 40°N-60°N (left) and Europe between 40°N-60°N and 20°W-40°E (right) for CNT (solid) as well as relaxed forecast, with relaxation region north of 70°N (R70, dashed), north of 80°N (R80, gray dotted) and in the Tropics (TROP, dash-dotted).

Generally the forecast error increases strongly with time, especially within the first 15 days, after that the curve of the mean error flattens. However, the absolute error of a single forecast can grow substantially; the flattening of the error curve indicates a saturation of the error and loss of predictive skill, i.e. forecast predicting a climatological value will not give a better result.

For all investigated areas, the relaxation above 70°N (R70) is much more efficient than the relaxation only above 80°N (R80). This can be easily explained because the area north of 70°N is approximately four times larger than the area north of 80°N. For the R70 twice as many grid points are relaxed, furthermore the signal from the Arctic has to travel a shorter distance before it reaches Europe.

Another important point is that the reduction of the forecast error is notably larger after day 15, which suggests that a better knowledge of the Arctic can improve the quality of the forecasts especially for the extended-range. The model used for producing the forecast is performing relatively well in the first 15 days. Therefore the relaxation cannot bring much improvement for this time range. Furthermore, the signal from the Arctic needs time to propagate south.

Comparing the impact of the relaxation in the Arctic to the impact of the relaxation in the tropics, R70 is more efficient than TROP for all three investigated areas, even though the area of the tropics is much larger. Comparing R80 and TROP, the latter leads to better forecasts in the mid-latitudes and in Europe. The fact that for the time window between day 15 and day 20 in Europe the error of TROP is as high as that of CNT can possibly be explained with an insufficient sample size, given that fewer grid points are averaged for Europe than for the mid-latitudes.

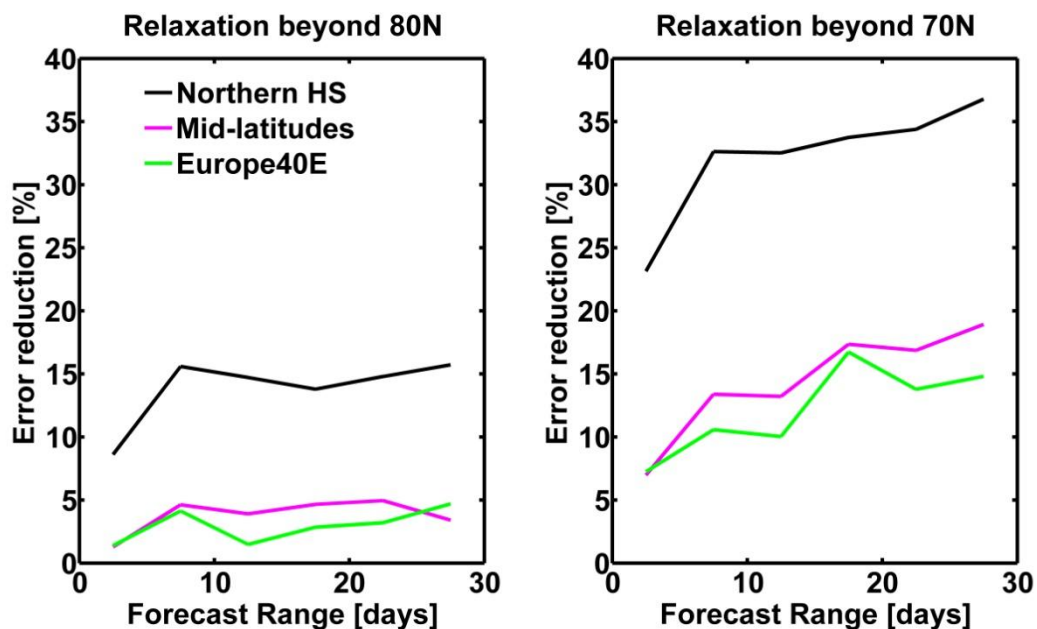


**Figure 6** Mean reduction of the forecast error after applying relaxation technique north of 70°N (left) and north 80°N (right), averaged over Northern Hemisphere Extratropics 40°N-90°N (black), Mid-latitudes between 40°N and 60°N (magenta) and Europe between 40°N and 60°N as well as 20°W and 40°E.

To quantitatively compare the effect of the relaxation on different areas, the mean error reduction  $\overline{ERed}$  for R70 and R80 is shown in **Figure 6**. It can be clearly seen again that the size of the relaxation area makes a large difference, as the error reduction for Europe is more than twice as large for R70 as for R80. Furthermore  $\overline{ERed}$  increases with the time of the forecast and for R70 reaches up to 15% for Europe and the mid-latitudes. For R80  $\overline{ERed}$  only increases within first 10 days and stays below 5% for the whole time range.

These results show that the relaxation north of 80°N is not very efficient for the mid-latitudes and Europe and therefore the further analysis is constrained to the relaxation north of 70°N.

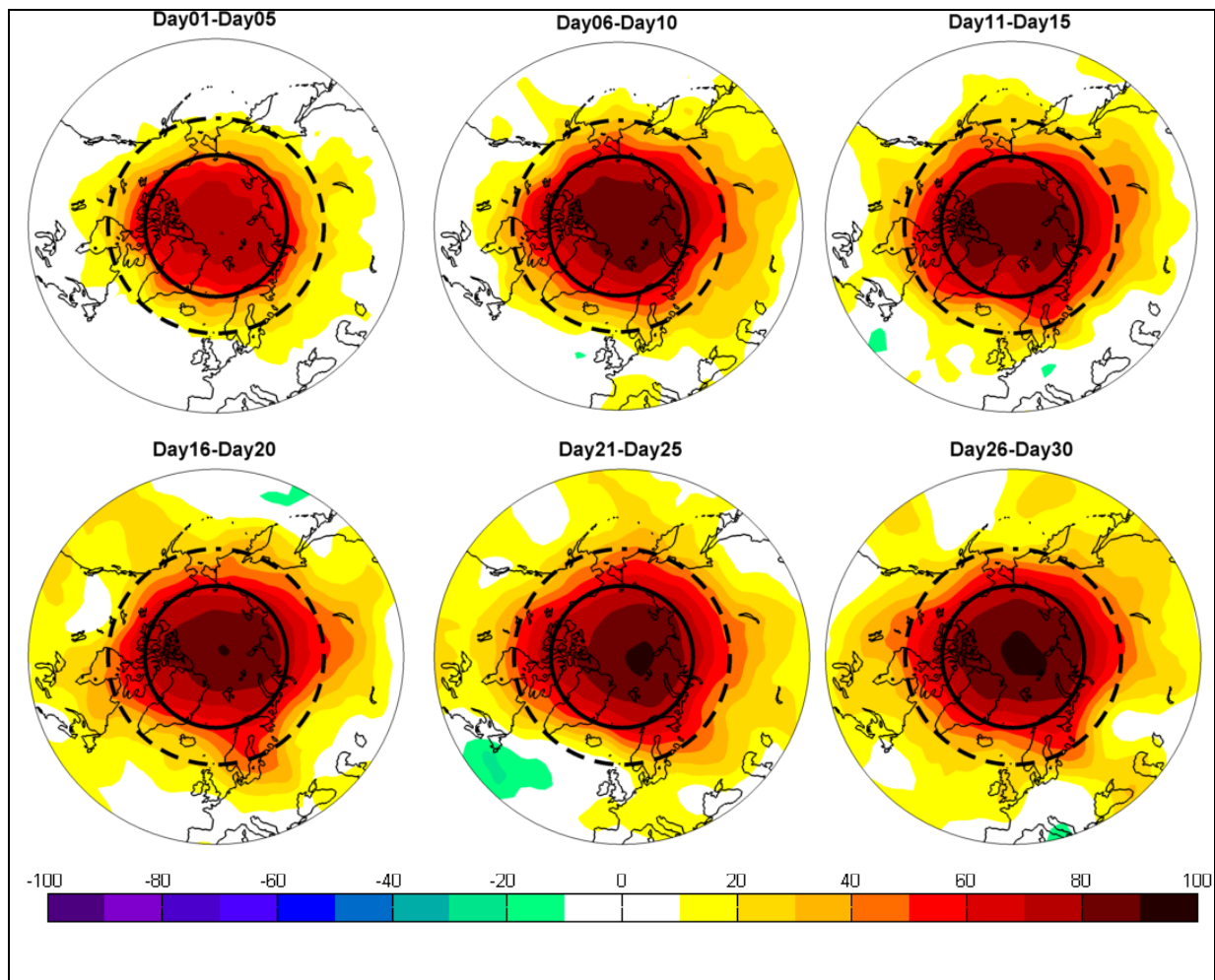


**Figure 7** Mean error reduction in % for winter-only experiment, for Northern Hemisphere Extratropics between 40°N -90°N after applying relaxation north of 70°N. Black solid line indicates the boundary of relaxation region (70°N), the dashed line 60°N.

The spatial structure of the error reduction for the NHE is shown in **Figure 7**. The relaxation approach clearly works, as in the relaxed region the forecast error is reduced by more than 80% already for the time window between day 6 and day10. With increasing time range of the forecast the signal is gradually propagating towards south and the  $\overline{FE}$  in remote regions decreases. It seems that the positive impact of the Arctic can be mainly observed over the continents, and not so much over the oceans. Probably due to sampling issues, for some time windows in some areas (e.g. in the Atlantic and the Pacific) the relaxed forecasts are worse than CNT.

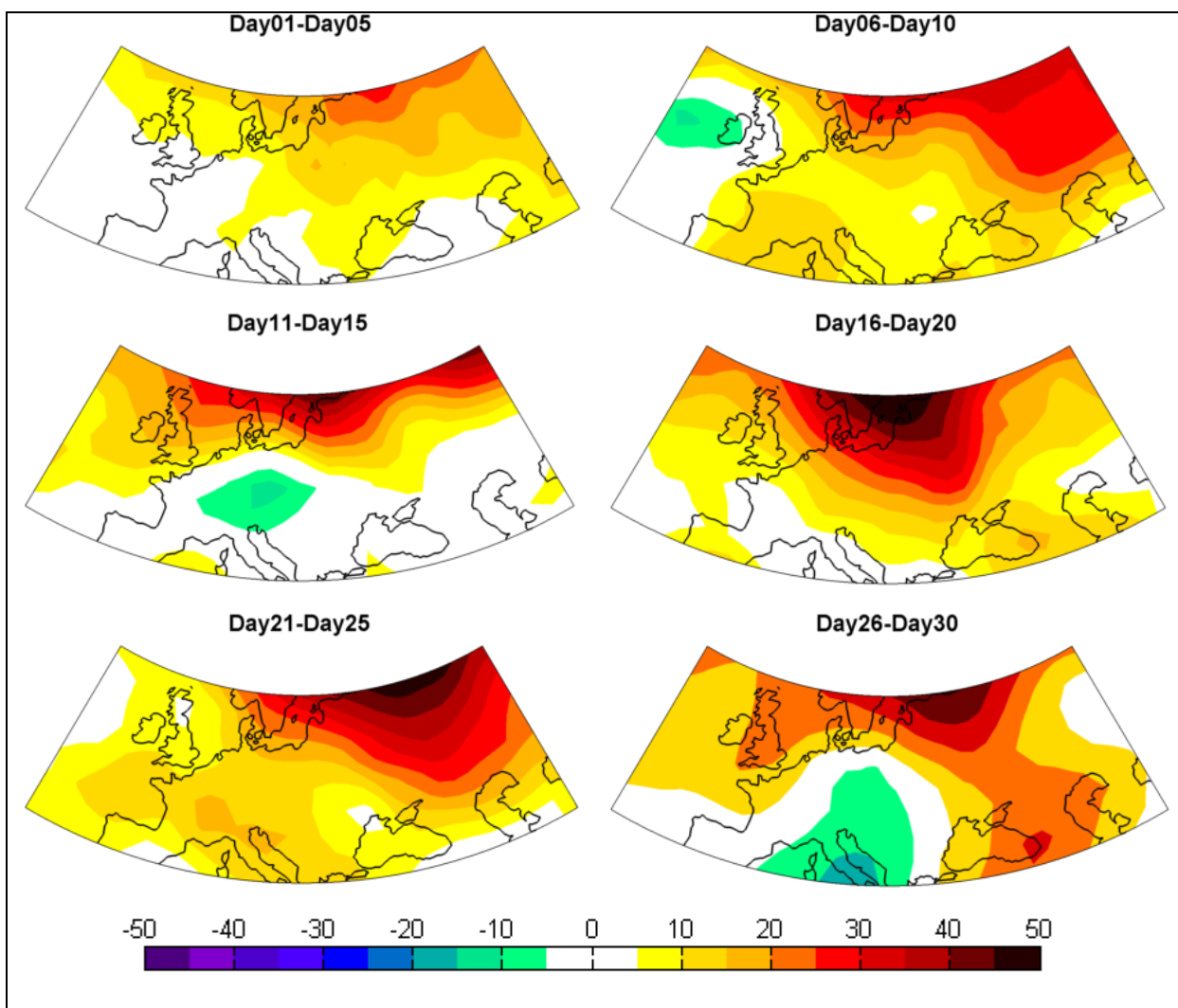


**Figure 8** Mean error reduction in % over European region between 40°N-60°N and 20°W-60°E for winter-only experiment for relaxation north of 70°N.

As the focus of this Thesis is on Europe, **Figure 8** shows the error reduction between 40N and 60 N and between 20W and 60E (a larger area than the one used for



calculation of  $\overline{FE}$  ). First it can be seen that there are large differences in this region. On the one hand in the continental part of Europe the forecast can be improved by up to 50%. On the other hand, in large parts, especially in western and southern Europe, R70 leads to worse or similar forecasts as CNT. This means that the positive impact of the Arctic is mainly limited to northern and eastern Europe. In western Europe the influence of the Atlantic seems to dominate influence of the Arctic.

#### 4.1.2 Flow dependence of the mean impact

Another important issue is whether the improvement of the weather forecast can be linked to certain atmospheric conditions. To investigate this issue the composite analysis was carried out, for Europe as described in Chapter 3.4.1. **Figure 9** (left) shows the results of the composite analysis within the first 15 days. Most relevant for Europe are positive values over the North Atlantic (between Iceland, Greenland, and eastern coast of Canada) and the negative values over western Siberia and southern France. Positive (negative) values indicate that for improved forecasts Z500 was higher (lower) than for worsened forecasts. Therefore, when the forecasts are improved, an anomalous north-easterly wind transporting air masses across Scandinavia is present. As this wind hits the continent it turns into a north-westerly wind bringing the cold Arctic air masses towards the Caspian and the Aral Sea, and into an easterly wind blowing across the British Isles towards the Atlantic. This result is consistent with the spatial patterns of the error reduction (**Figure 7**, **Figure 8**) as the largest error reduction was also observed south of Scandinavia. Over the Atlantic Ocean the prevailing westerly wind reduces the impact of the Arctic.

The composite analysis produced for the simulated fields from the relaxation experiment instead of re-analysis fields (shown in the Appendix), shows very similar structures, as within 15 days the relaxed and observed field remain very similar. The pattern observed in **Figure 9** (left) also resembles the structure of the negative phase of the NAO, with positive anomalies over Iceland, and negative anomalies over south-western Europe. This was expected, as while NAO is negative, the westerlies are weaker and the cold air from Siberia is determining more the weather in Europe.

Strong signals are also present in other regions, that are more remote to Europe. The signal over the north- east Pacific is even stronger than the signal close to

Europe. Weaker signals are found over north-eastern Asia (negative) and central Asia (positive).

It should be noted that the variability of Z500 within the forecast errors for improved and worsened forecasts (see **Figure 2**), as well as within the corresponding re-analysis fields was high. The standard deviation within the “good” and “bad” re-analysis fields was actually larger than the difference of the means. The statistical significance was calculated with the Mann-Whitney ranksum test, the result for each grid point is shown in the **Figure 9** with the gray stars for the 95% level. Most of the differences are not statistically significant. Mostly only the grid points with the highest values are found to be significant, but significant values are found also in the regions south-west of Greenland and north of Iceland. The negative differences over Siberia and eastern Europe are not statistically significant. This shows that the variability and the randomness of the atmosphere are high and to make more conclusive statements, a larger data set would be desirable.

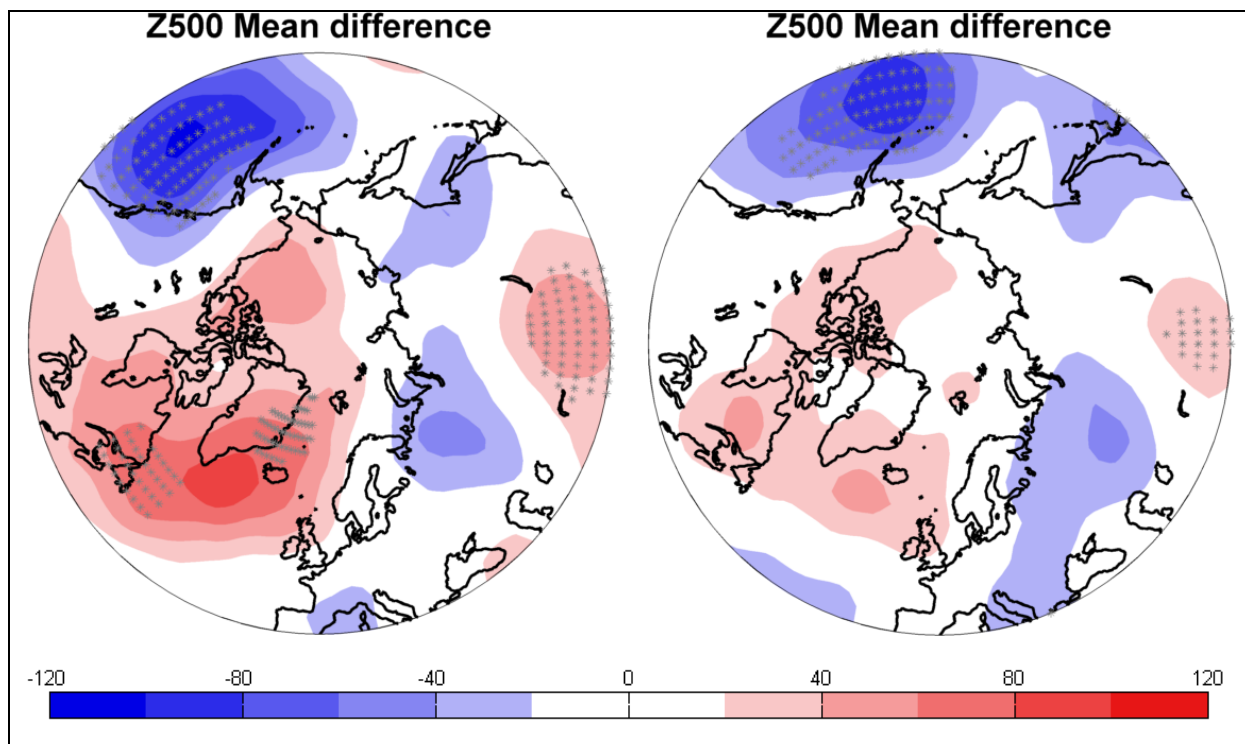


**Figure 9** Difference of the means of re-analysis fields (500hPa geopotential height in m) between improved and worsened forecasts over Europe for day1-day15 in winter. Statistically significant grid points (Mann-Whitney ranksum test) are shown with gray stars. The mean of improved and worsened forecasts was calculated of 5-day (left) or 3-day averaged (right) data.

Considering the second half of the forecast range (day 16- day30) the results of the composite analysis for re-analysis and relaxed fields differ. The relaxed field shows a pattern similar to the one for day1-day15, but the positive anomaly is spread over all of Europe, however a weak anomalous southward air flow is present over eastern Europe. The observed field shows a pattern resembling the NAO negative phase with a strong south-easterly flow (see Appendix). The reason for that is that beyond day 15 the difference between the re-analysis and relaxed fields is large. Furthermore also the noise level increases.

#### 4.1.3 Arctic versus tropics

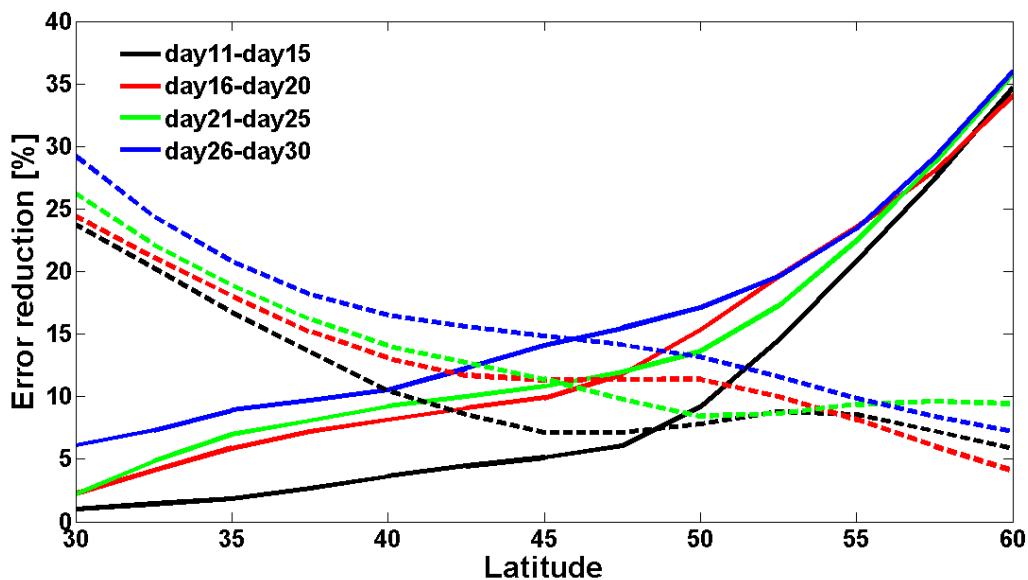


**Figure 10** Zonally averaged error reduction in % as a function of latitude between 30°N and 60° for the relaxation above 70°N(solid) and in the tropics (dashed) between 20°S and 20°N.

Already the first plots of the mean forecast error  $\overline{FE}$  for (**Figure 5**) show that the impact of the Arctic on the mid-latitudes is comparable to the impact of the tropics. Even though the area of the Arctic is much smaller, R70 is much more effective for all three investigated areas. Another very interesting issue is at which latitude the influence of the Arctic becomes stronger than that of the tropics. **Figure 10** shows the zonal average of the error reduction for the R70 (solid) and TROP (dashed) between 30°N and 60°N (for both starting 10° away from the relaxation boundaries), for the 5-day windows beyond day10 as within the first 10 days the effect of relaxation the is

small. As expected, for both experiments  $ER_{red}$  decreases as the distance from the relaxation region increases. However, close to relaxation region it is higher for R70 than for TROP, e.g.  $10^\circ$  from the relaxation region the mean error reduction after 30 days is 30% for TROP (at  $30^\circ\text{N}$ ) and 35% for R70 (at  $60^\circ\text{N}$ ). On the other hand, far from the relaxation region, it is lower for R70 than for TROP, especially for the shorter time range, e.g. for time window between day 11 and day 15,  $40^\circ$  away from the relaxation boundaries it is approx. 6% for TROP (at  $60^\circ\text{N}$ ) and close to zero for the R70 (at  $30^\circ\text{N}$ ). Furthermore, close to the relaxation region the error reduction for R70 seems to depend less on the considered time window, as north of  $55^\circ\text{N}$  the curves for different days are close together.

The point where the mean influence of the Arctic is as strong as that of the tropics depends slightly on the considered time window: for day11-day15 it is located at approx.  $48^\circ\text{N}$  and it shifts slightly towards  $46^\circ\text{N}$  for day26-day30. In the mid-latitudes, as defined in this study, the impact of the Arctic appears to be stronger than the impact of the tropics. Only in the southern approx.25% of the mid-latitudes the impact of the tropics dominates.

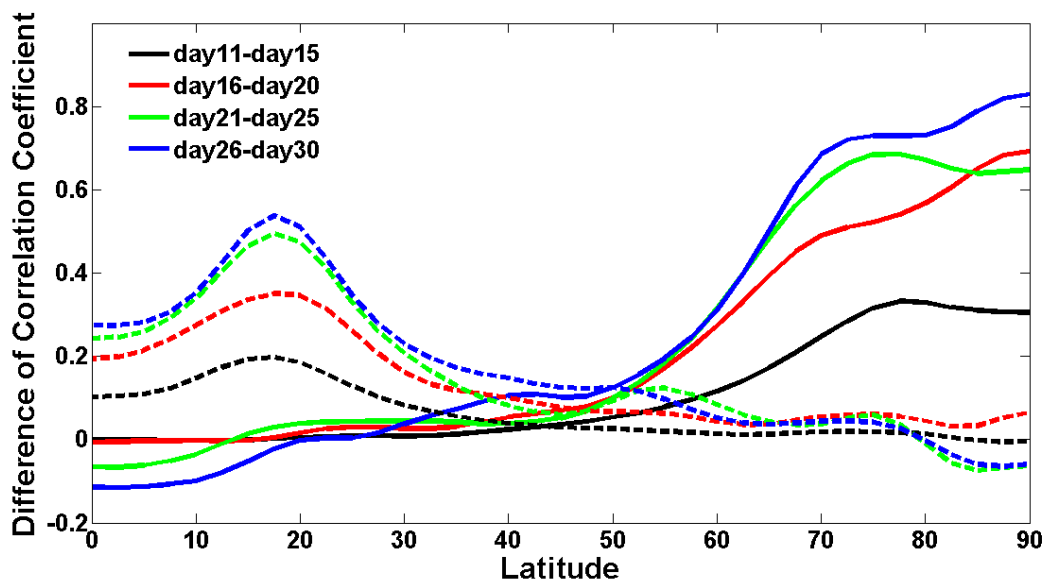


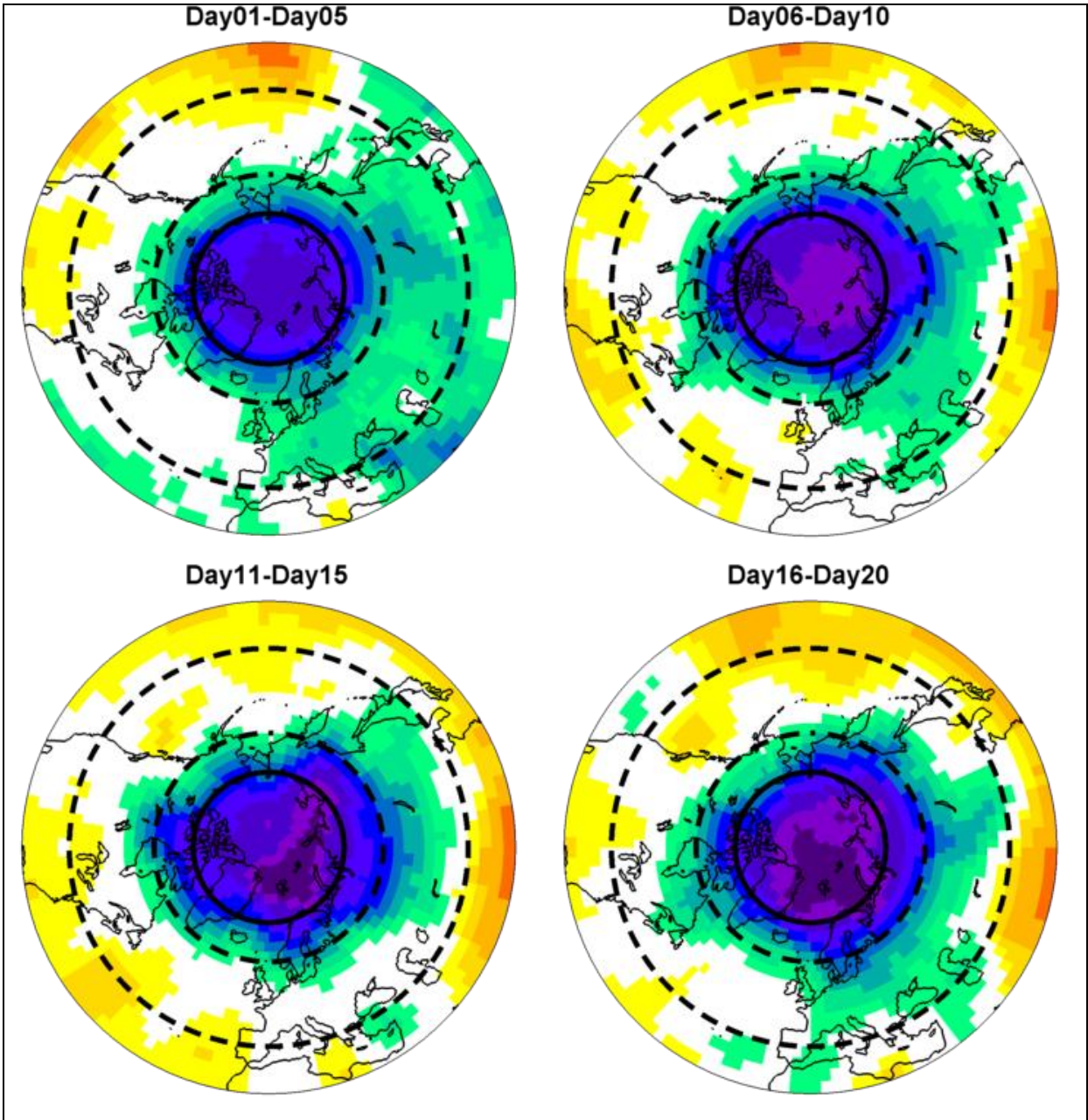
**Figure 11** The difference of zonally averaged correlation coefficient between forecast relaxed north of  $70^\circ\text{N}$  and CNT (solid) as well as between forecast relaxed in the tropics between  $20^\circ\text{S}$  and  $20^\circ\text{N}$  and CNT (dashed). The correlation coefficient was calculated for each grid point between the forecast and the re-analysis.

A second diagnostic parameter is the zonal average of the correlation coefficient. To account only for the improvement due to the relaxation, **Figure 11** shows the

difference of the correlation coefficient between R70 and CNT as well between TROP and CNT. The model has very good predicting skills for the tropics where the absolute correlation coefficient is 0.7 for day11-day20 (shown in the Appendix). Therefore the relaxing in this region improves the correlation coefficient only by approx.0.3. But the model is much less efficient in predicting the weather of the extratropics and Polar Regions where the absolute correlation coefficient is 0.2 for day16 –day20. Therefore it is not surprising that relaxation in the Arctic increases the correlation coefficient considerably, especially for later time windows. For day26-day30 the correlation coefficient increases by 0.8. But, it should be mentioned, that the correlation coefficient is not linear, so the increase by 0.8 is much more efficient than by only 0.3.

Similar to the error reduction, also the correlation coefficient difference decreases with increasing distance from the relaxation area. However for both, TROP and R70 the improvement for the mid-latitudes is rather small. The intersection of the two curves is again between 40°N and 50°N, which also corroborates that the relaxation of the Arctic is more effective in reducing the error of the weather forecasts for mid-latitudes.

To compare the influence of the tropics and the Arctic on NHE the difference of *ERed* between TROP and R70 is shown in **Figure 12** (southern boundary of NHE is extended to 30°N) with negative difference indicating that *ERed* due to relaxation of the Arctic is higher. Obviously the impact of the Arctic is higher in almost all of Europe with the exception of the Atlantic region and the Mediterranean region. However, when the whole mid-latitudes are concerned, the tropics are more important than the Arctic for North America, the Atlantic and the Pacific.





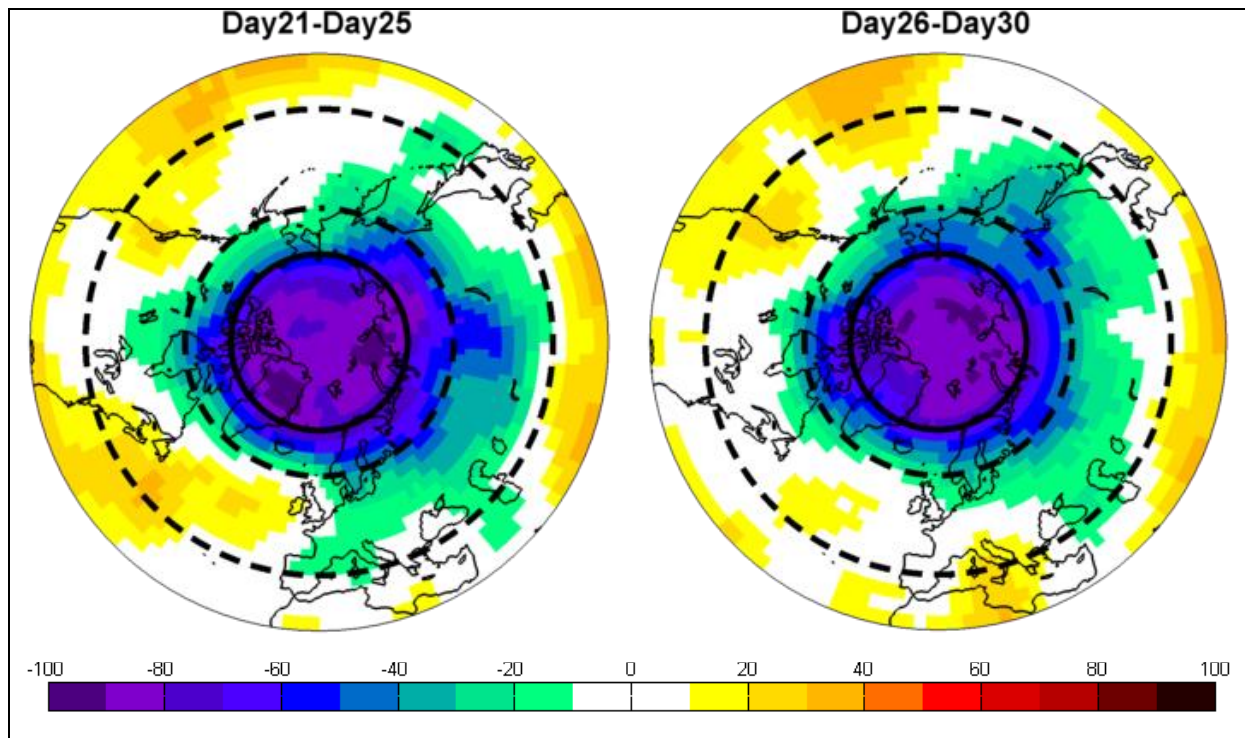


**Figure 12** The difference of the error reduction in % between the relaxation in the tropics (20°S-20°N) and in the Arctic (70°N-90°N). The negative difference means that the relaxation in the Arctic is more effective in reducing the forecast error. The solid line indicate the 70°N, the dashed lines indicate boundaries of mid-latitudes (40°N-60°N).

#### 4.1.4 Sensitivity test

The results presented so far suggest that there is a link between the Arctic and the weather in Europe; moreover, this link seems to be stronger for the negative phase of NAO. To obtain the results, some parameters needed to be defined e.g. averaging length as 5 days. To have a large data set, the data from 22 years were analyzed, which a relatively long time is considering the changes of the climate in the last decades. Therefore some further analyses were done with changed parameter choice to test if the results obtained so far are robust.

##### A) 3 day averages

Using 3day windows for averaging generally increases the forecast error, as extreme values are not eliminated from the average (the noise is higher). However, the general result obtained from error reduction does not change when 3day windows are used (**Figure 13**).

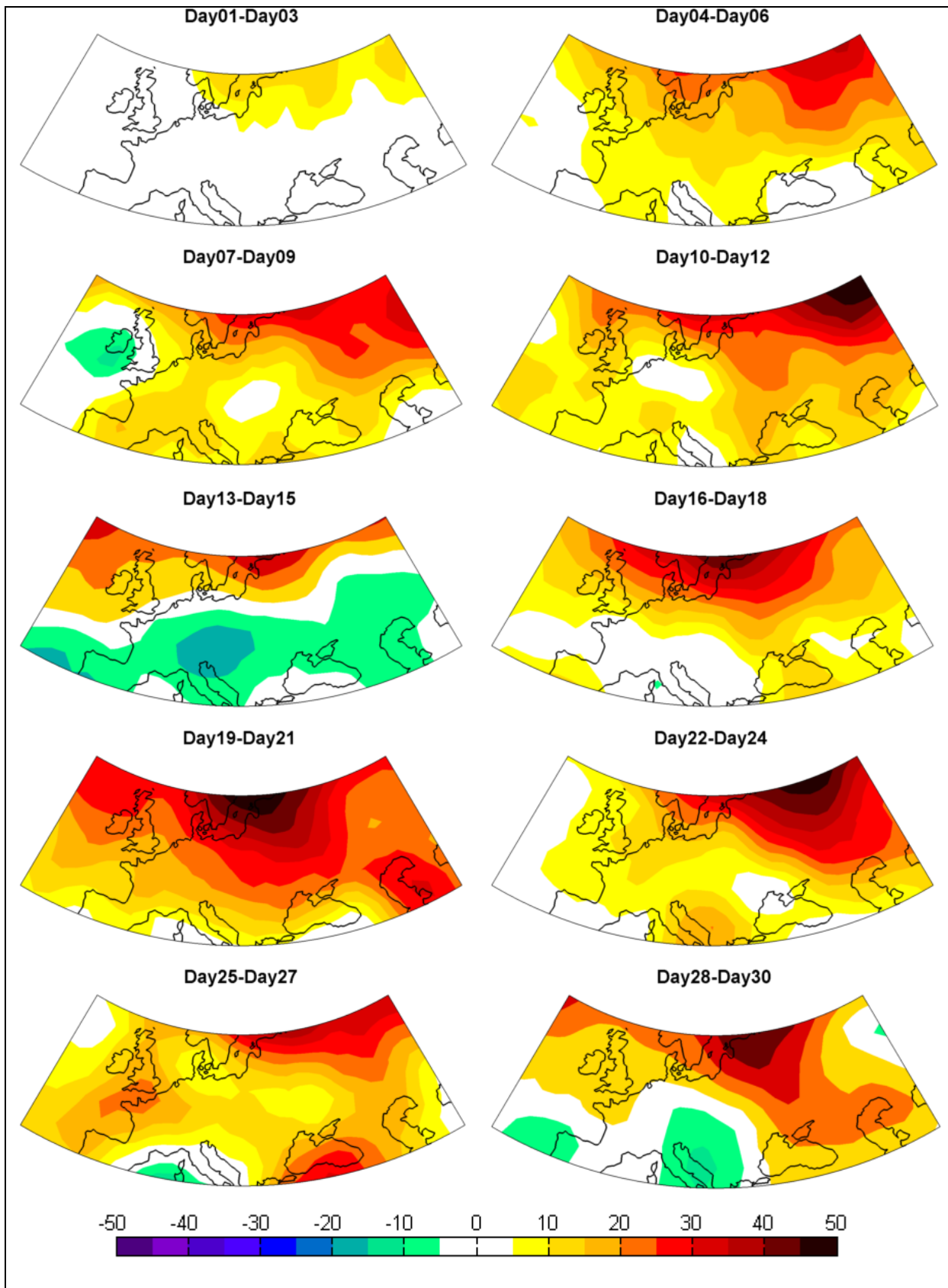


**Figure 13** Mean error reduction in % over European region between 40°N-60°N and 20°W-60°E for winter-only experiment, calculated as 3-day average.



The range of the error reduction for Europe remains the same as for the 5day average, with the highest improvement occurring over northern and eastern Europe. But more of the daily variability can be captured and some new features are visible, e.g. an increased error reduction over the Atlantic region for day 19-day 21 and day 25-day 27, which may be by chance. Furthermore, it can be clearly seen from the day 1-day 3 window that 3 days are too short for the relaxation to bring much of an improvement.

The composite pattern (**Figure 9**, right) shows in general the same structure as for the 5-day windows, but the magnitude of the differences and their statistical significance decrease.

### *B) Definition of Europe*

Another interesting question is how the result will change with a modified definition of Europe, as the error is most strongly reduced over the continent. To investigate this question, Europe was divided into a maritime Western (EUR-W, 20W to 20E, red) and a continental Eastern (EUR-E, 20E to 60E, green) part. The mean forecast error  $\overline{FE}$  was calculated for each region separately (**Figure 14**).  $\overline{FE}$  of CNT is slightly highest for EUR-W and  $\overline{FE}$  is the lowest for EUR-E. This shows that the predictability is higher over the continent.

Also the effect of the relaxation is also sensitive to the definition of the region:, for the R70 the effect is comparable for EUR-W and whole of Europe. However, as  $\overline{FE}$  of CNT for EUR-W is the highest, so is  $\overline{FE}$  with the relaxation. On the other hand, for EUR-E R70 is slightly more efficient, and above all the positive effect starts earlier, as already at day10 the error is substantially reduced. As shown in the previous section, the impact of the tropics is limited to EUR-W. Therefore it is not surprising, that the mean effect of the tropics on EUR-E is very weak. For EUR-W the impact of the tropics is visible, but, the weaker than the one of the Arctic.

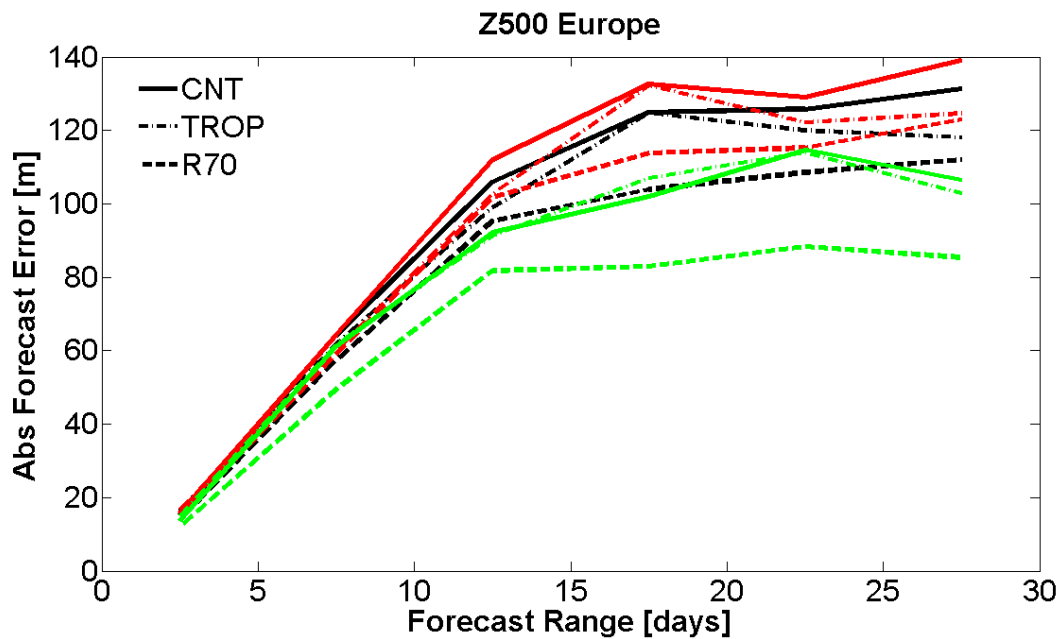


**Figure 14** Mean absolute error of 5-day-averaged forecasts of 500hPa geopotential height fields (m) over whole Europe between 40°N-60°N and 20°W-40°E (black) as well as maritime, western Europe between 20°W and 20°E (red) and continental, eastern Europe between 20°E and 60°E (green); for CNT (solid) as well as relaxed forecast, with relaxation region above 70°N (R70, dashed) and in the Tropics (TROP, dash-dotted).

The results of the composite analysis for EUR-W and EUR-E are shown in **Figure 15**. For EUR-W the positive anomaly is found over the North Atlantic, Greenland and central Arctic while the negative anomaly is over west Siberia (as for whole of Europe) and central Europe. The anomalous north-easterly flow is found over Scandinavia, the North Sea and the British Isles. For EUR-E the pattern is different, as the positive anomaly is over Iceland, Scandinavia and the Barents Sea leading to an anomalous easterly flow. Therefore the result of the study is very sensitive to the definition of Europe. Considering only eastern or western Europe instead of the whole Europe leads to quite different conclusion. However, even though no direct impact of the Arctic is observed for EUR-E, the Siberia seems to be important.

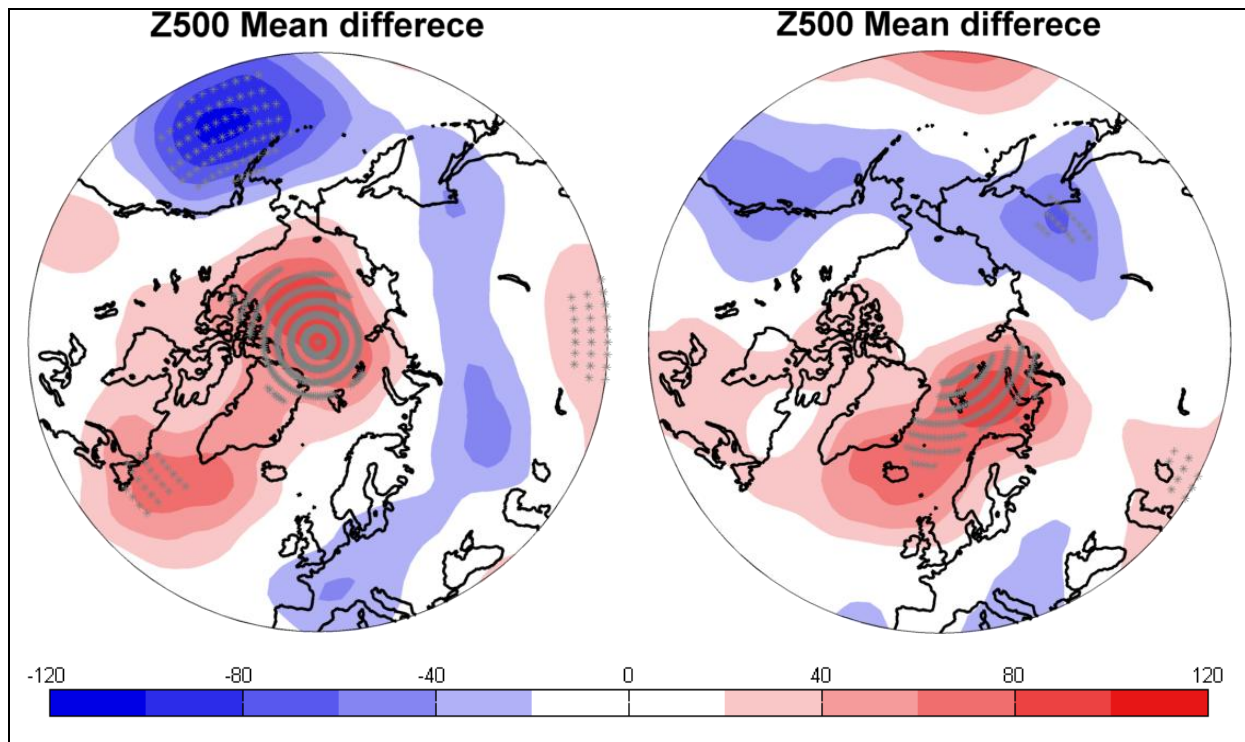


**Figure 15** Difference of the means of re-analysis fields (500hPa geopotential height in m) for day1-day15 in winter between improved and worsened forecasts for western Europe (20°W-20°E, left) and eastern Europe (20°E-60°E, right). Statistically significant grid points (Mann-Whitney ranksum test) are shown with gray stars.

## 4.2 All-seasons medium range forecasts

The results of the winter-only experiment show that the better knowledge of the Arctic can improve the quality of the weather forecast for Europe, but the signal to noise ratio is high. To improve statistical significance, the experiment was repeated with larger sample size. Furthermore, the investigations were extended over whole year to investigate the seasonality of the link between the Arctic and Europe.

### 4.2.1 Mean impact

The mean forecast error averaged over Europe is shown in **Figure 16** for all four seasons for CNT (solid) and forecast relaxed north of 75°N and 75°S (R75, dashed). Firstly, the mean forecast error strongly depends on the season: after 14 days  $\overline{FE}$  is almost twice as large for winter as for summer. Secondly, the error is increasing with time of the forecast and no saturation is reached yet. “Lower predictability” of the weather in Europe in winter can be explained with higher variability in the

atmosphere. In winter the meridional temperature gradient between the tropics and the Polar Regions is stronger and as a consequence and the exchange of the air

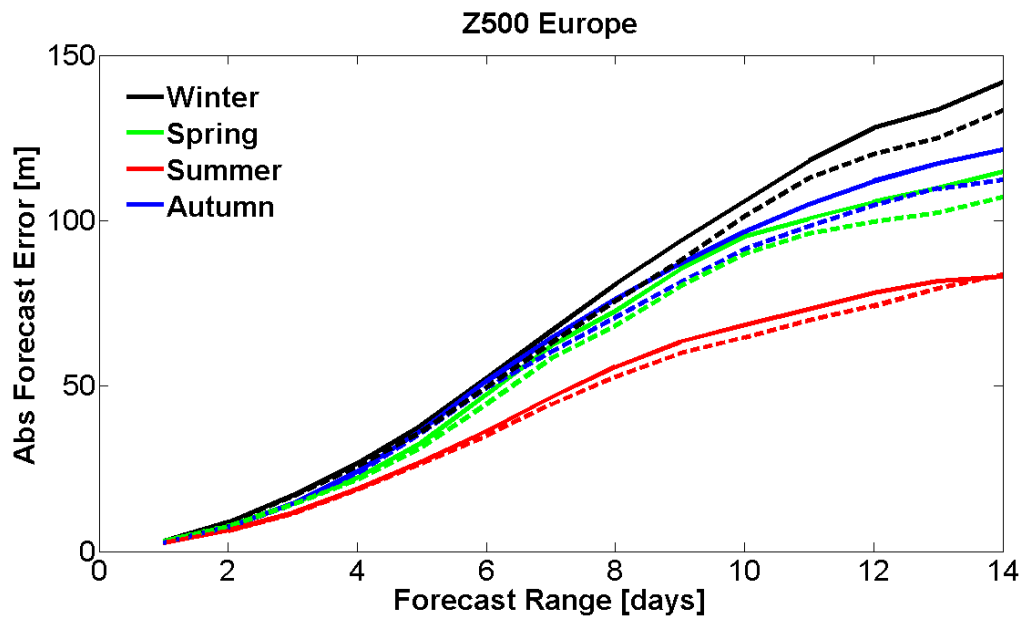


**Figure 16** Mean absolute error of 1-day-averaged forecasts of 500hPa geopotential height fields (m) over Europe for CNT (solid) and forecast relaxed over 75°N (dashed) for winter (black), spring (green), summer (red) and autumn (blue).

masses is enhanced by the more frequent development of fronts and eddies. Furthermore in summer the anomalies are smaller, therefore the mean error also is smaller.

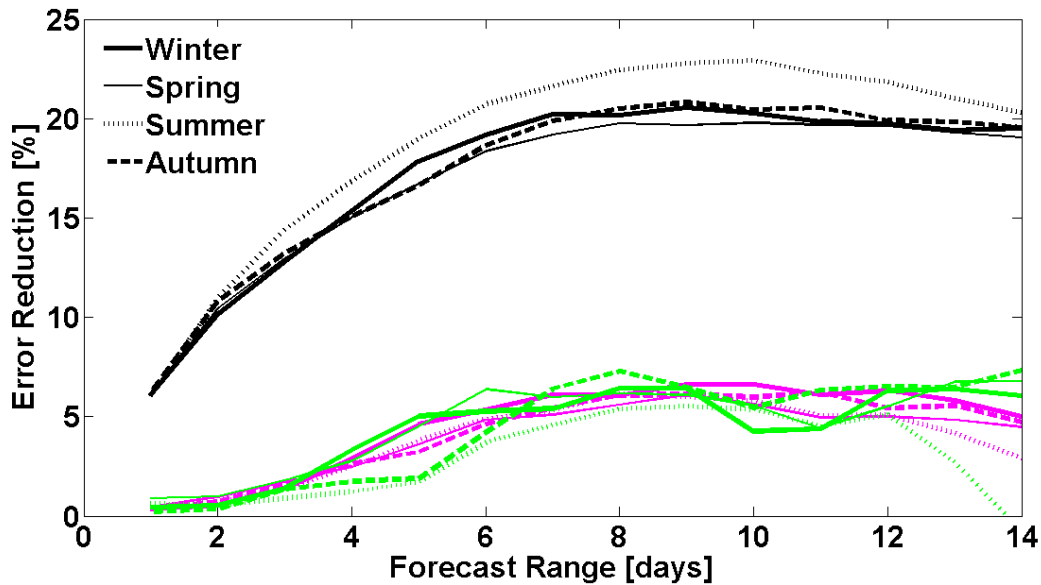


**Figure 17** Mean error reduction after applying relaxation north of 75°N, averaged over Northern Hemisphere Extratropics (40°N-90°N, black), Mid-latitudes (40°N-60°N, magenta) and Europe (40°N-60°N and 20°W-40°E, green), for winter (solid, thick), spring (solid, thin), summer (dotted) and autumn (dashed).

Compared to the first set of experiments, the errors in the all-seasons experiments is higher as averaging length (24h) is much shorter and, thus the synoptic variability better captured. Low pressure systems that determine the daily variation are not filtered out and increase the mean absolute error.

The error reduction (**Figure 17**) depends strongly on the investigated region and the time range of the integration. The improvement of the forecast increases until approx. day 6 and from that point it stays relatively stable. It is strongest for the entire NHE with approx. 18% and already on day1 the error is reduced by 5 % (as the relaxation area is included). For mid-latitudes (magenta) and Europe (green) the improvement within the investigated time of 14 days is only approx. 5% and almost no improvement can be observed in the first 2 days. Compared to the winter-only experiments, the error reduction of R70 for the first 14 days is approximately halved, the main reason being that the area of relaxation is smaller (north of 75°N compared to 70°N in R70). Furthermore, in the second set of experiments the averaging length is smaller (24 hours instead of 5 days) and the daily variation of Z500 is contributing more to the mean absolute error. Considering the variability between the forecast days, the curves for NHE and mid-latitudes are smoother than for Europe, as the area of Europe is much smaller and therefore sampling is more of an issue.

If the seasons are considered, there are not much differences between them, however, two features merit attention: the error reduction in summer for Europe is slightly lower than for other seasons and strongly decreasing from day 12. For the NHE, however the error reduction is the largest in summer. This means that the relaxation in summer is not bringing much improvement for Europe and mid-latitudes, but the forecasts for Polar Regions may be improved.

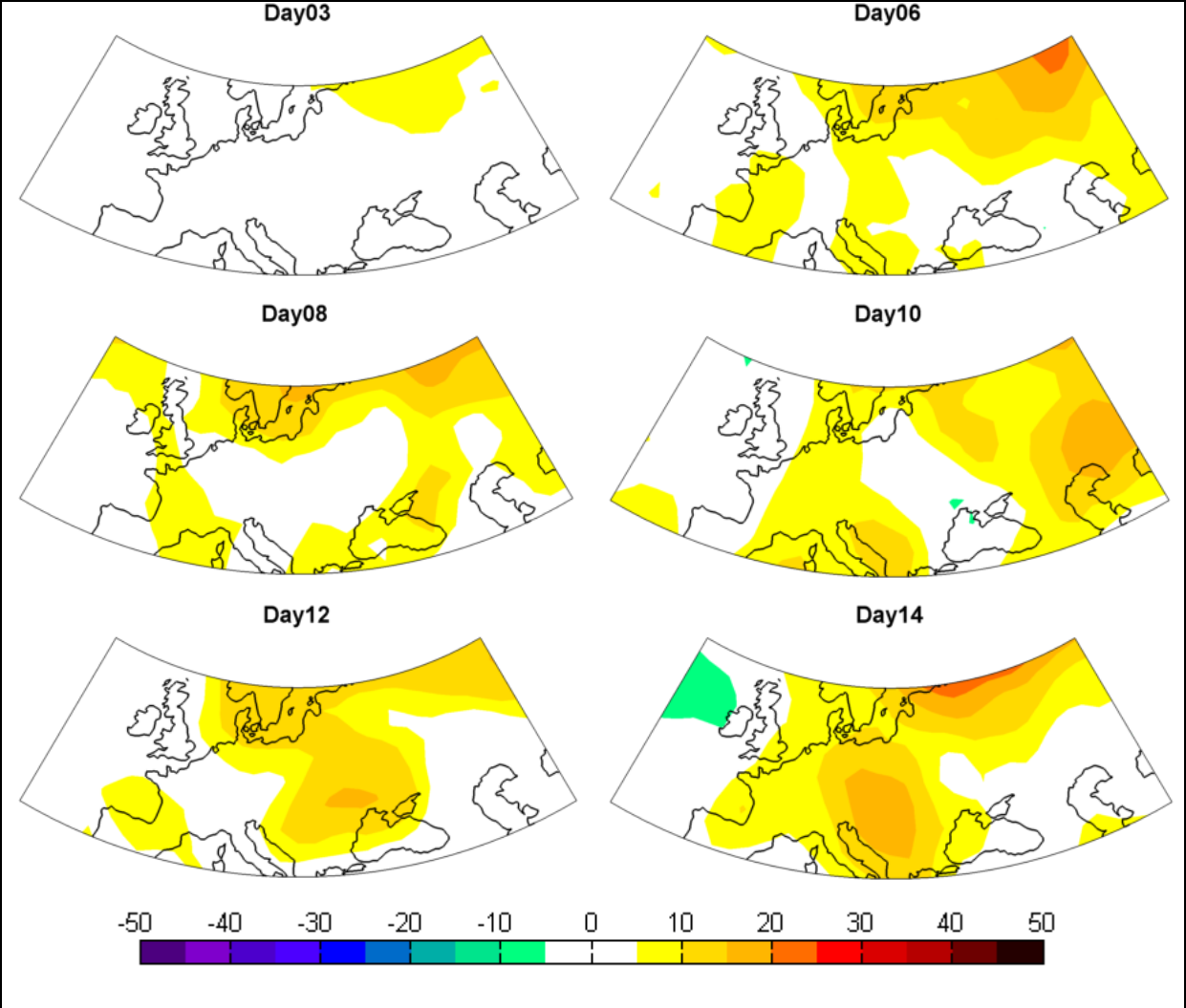


**Figure 18** Mean error reduction in % over European region between 40°N-60°N and 20°W-60°E for winter (DJF).

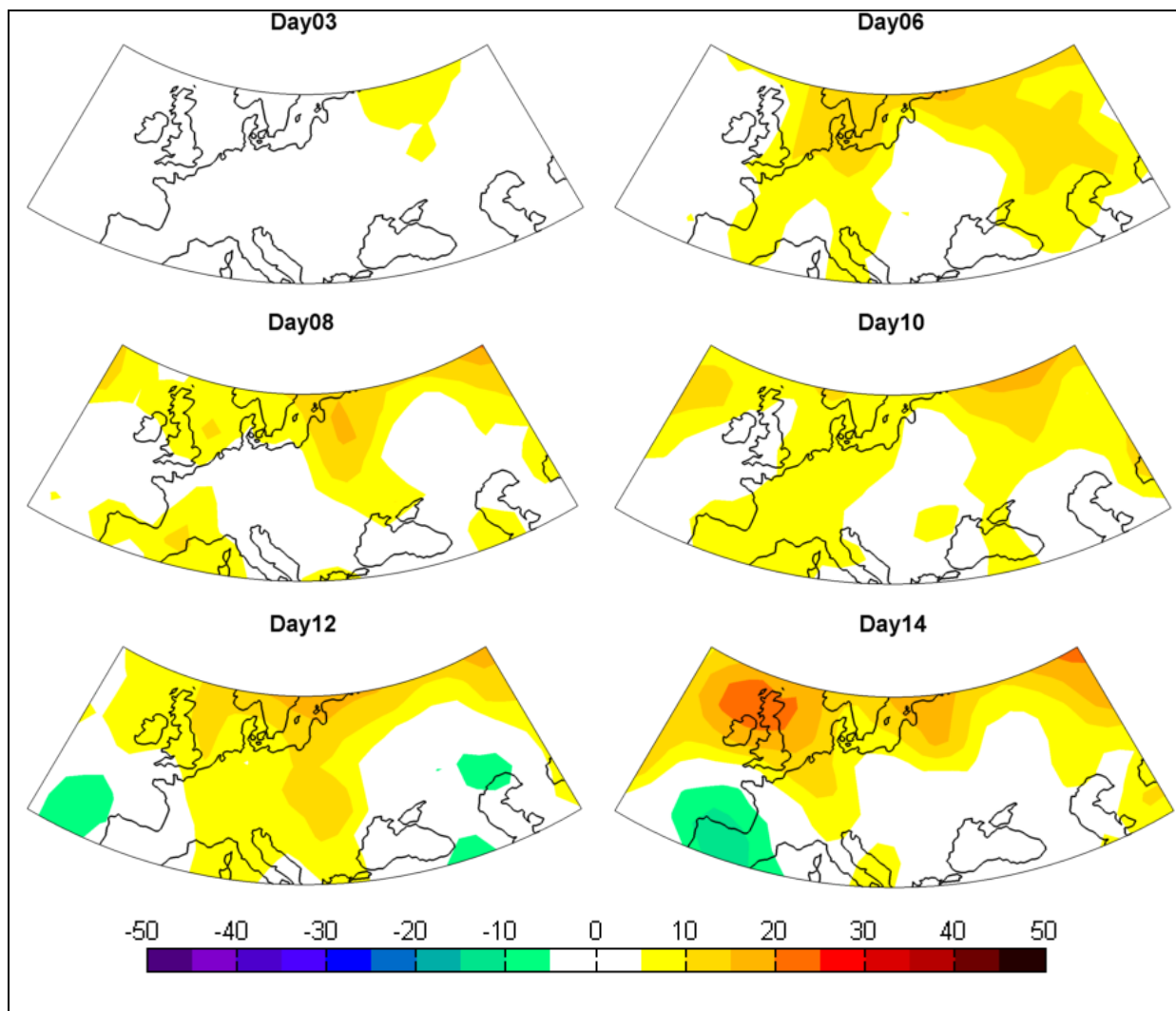


**Figure 19** Mean error reduction in % over European region between 40°N-60°N and 20°W-60°E for spring (MAM).

*ERed* is plotted for Europe in (**Figure 18**, **Figure 19**, **Figure 20**, **Figure 21**) for some chosen forecast days to examine whether the spatial structure changes for different seasons. Generally, the biggest improvement can be observed in north-eastern Europe, as for the winter-only experiments, where it reaches up to a maximum of 30%. Some areas in southern Europe show again that CNT was a better forecast. The variability between single forecast days is very high which emphasizes again the low signal to noise ratio of the system.

Comparing the seasons, it seems that the error reduction is slightly lower in summer (**Figure 20**) and autumn (**Figure 21**) than in winter (**Figure 18**) and spring (**Figure 19**). Moreover, in winter and spring the effect of the relaxation propagates faster towards south, as on day 6 larger areas have an error reduction above 5%. Furthermore, looking closer at the Atlantic region, especially for the British Isles

(approx. 20W -2E) some seasonal changes can be observed. This region has very low or even negative error reduction for winter (in both sets of experiments), but higher error reduction in other seasons, especially in spring (day 14) and autumn (day 14), but also for a few days in summer. This can also be observed for Spain, but not so often. This shows that in winter in western Europe the westerlies, that are also particularly strong in winter, are much more important than the cold air coming from the Arctic. In other seasons when the westerlies are not that strong, the relative impact of the Arctic is higher.

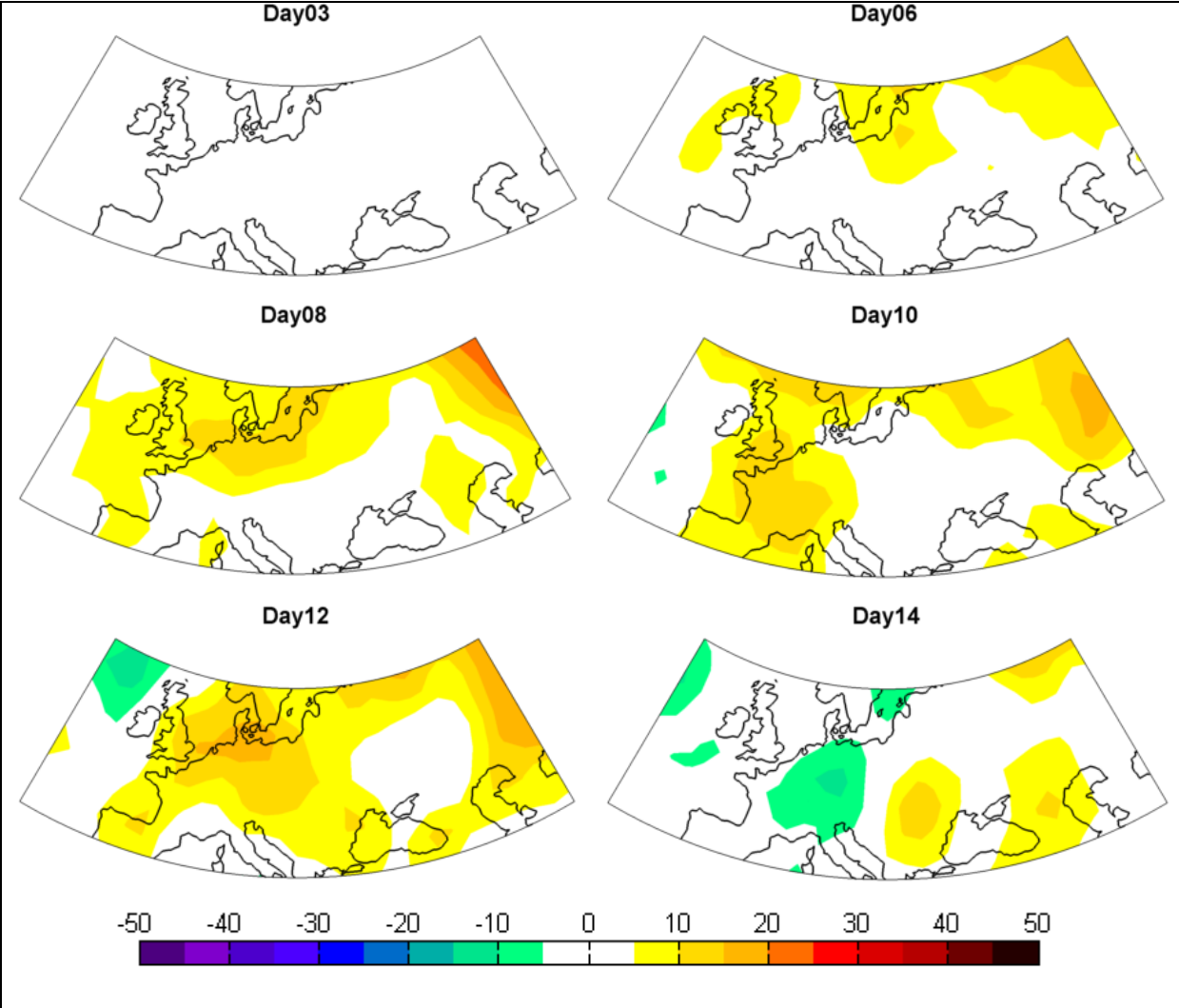


**Figure 20** Mean error reduction in % over European region between 40°N-60°N and 20°W-60°E for summer (JJA).



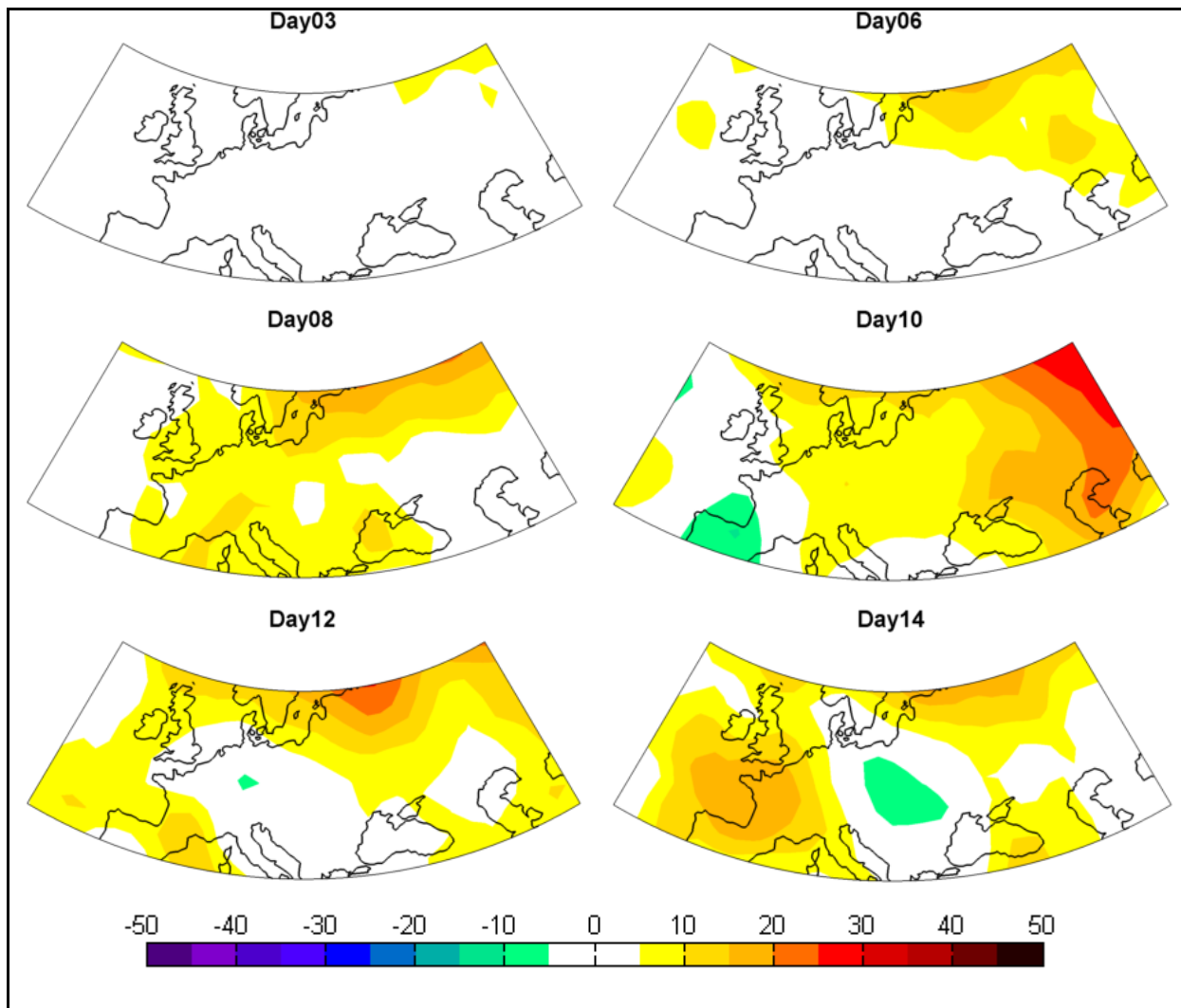


**Figure 21** Mean error reduction in % over European region between 40°N-60°N and 20°W-60°E for autumn (SON).

#### 4.2.2 Flow dependence of the mean impact

Also for all four seasons the composites of the re-analysis fields were analyzed. The means of re-analysis fields for Z500 (m) for improved and worsened forecast for Europe were calculated over 14 days. The difference of the means is shown in **Figure 22** and large difference between seasons can be observed.

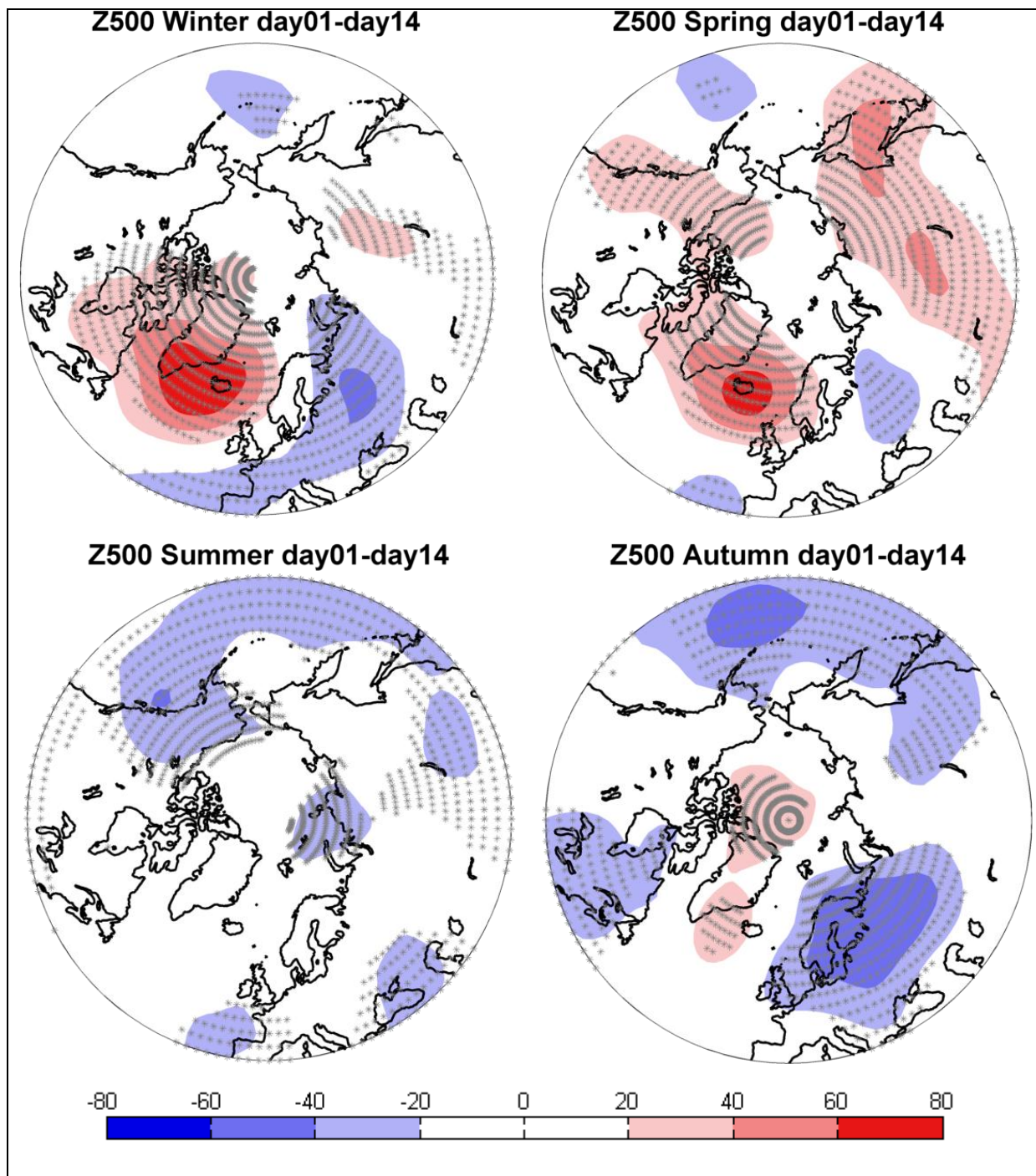


**Figure 22** Difference of the means of re-analysis fields (500hPa geopotential height in m) between improved and worsened forecasts over Europe for day1-day14. Statistically significant grid points (Mann-Whitney ranksum test) are shown with gray stars. data

The figure for winter resembles the figure for the winter-only experiment, however, while the signal is slightly weaker, it has higher statistical significance. The positive anomaly center is shifted towards the east (North Atlantic, Iceland, south-east Greenland), while the negative center is approximately at the same location, with extension into southern Europe. Furthermore the anomalies over the North Pacific

and East Asia are much weaker than in the winter-only experiment. The resulting anomalous air flow transports the cold arctic air across Scandinavia and then towards the west along the North Sea and towards the east into Siberia.

Similar patterns are found for spring and autumn, but not for summer when only small (up to 40m) negative anomalies can be observed in southern Europe. Therefore no strong air flow anomalies can be distinguished in summer. This is consistent with previous results from this study, as in summer the error reduction in Europe due to relaxation in the Arctic is lower. In spring the pattern is shifted eastward, a positive anomaly is well developed over Iceland, but the negative anomaly over eastern Europe is weaker. The cold arctic air is transported across Scandinavia, similar as in winter. Furthermore negative anomalies are found over south Atlantic, resembling again the negative phase of the NAO. In autumn, the positive center is located at the south tip of Greenland and is much weaker compared to winter, but the negative center is stronger and bigger than in winter (Scandinavia, north-eastern Europe). The resulting anomalous southward flow is shifted to the west, between Scandinavia and Greenland, and then turns to the south–east over the British Isles and Germany.

Comparing this figures with the error reduction, usually the strongest improvements of the forecast correspond to strong Z500 anomalies in the composite (in winter negative anomalies in northern and eastern Europe; in the spring positive anomalies over the British Isles) and to the flow direction (in spring the south coast of the North Sea, easterly flow is observed). As no strong flow anomalies are present in summer, the error reduction cannot be linked to the atmospheric conditions. In autumn the dependence is also not very strong. Though  $ER_{red}$  is high for most parts of Europe, for day 12-day 14 in central Europe the relaxed forecast are even worse. For that time anomalous north-western wind can be observed that will enhance the westerlies, transporting the moist air from Atlantic.

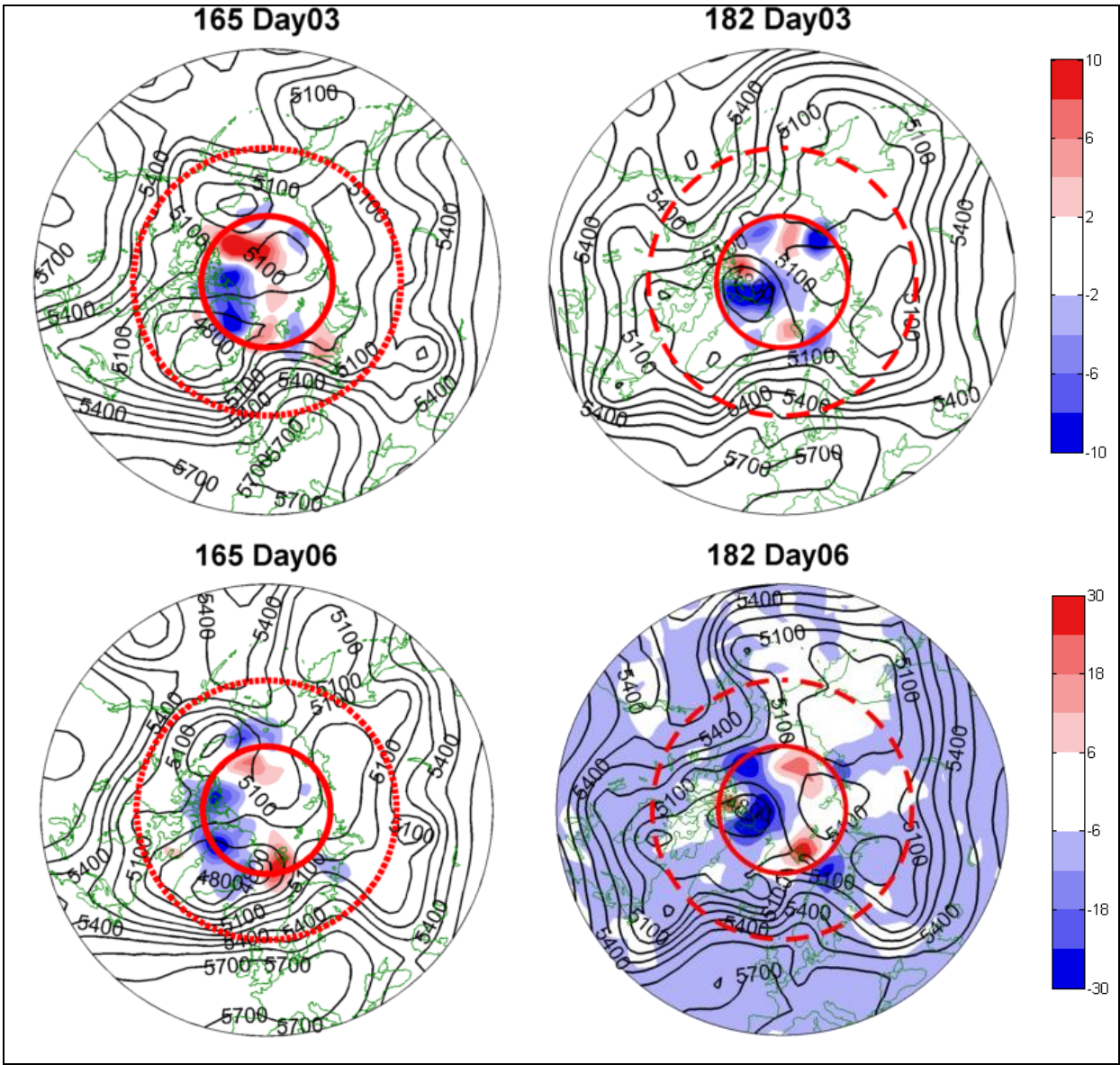
#### 4.2.3 Case examples

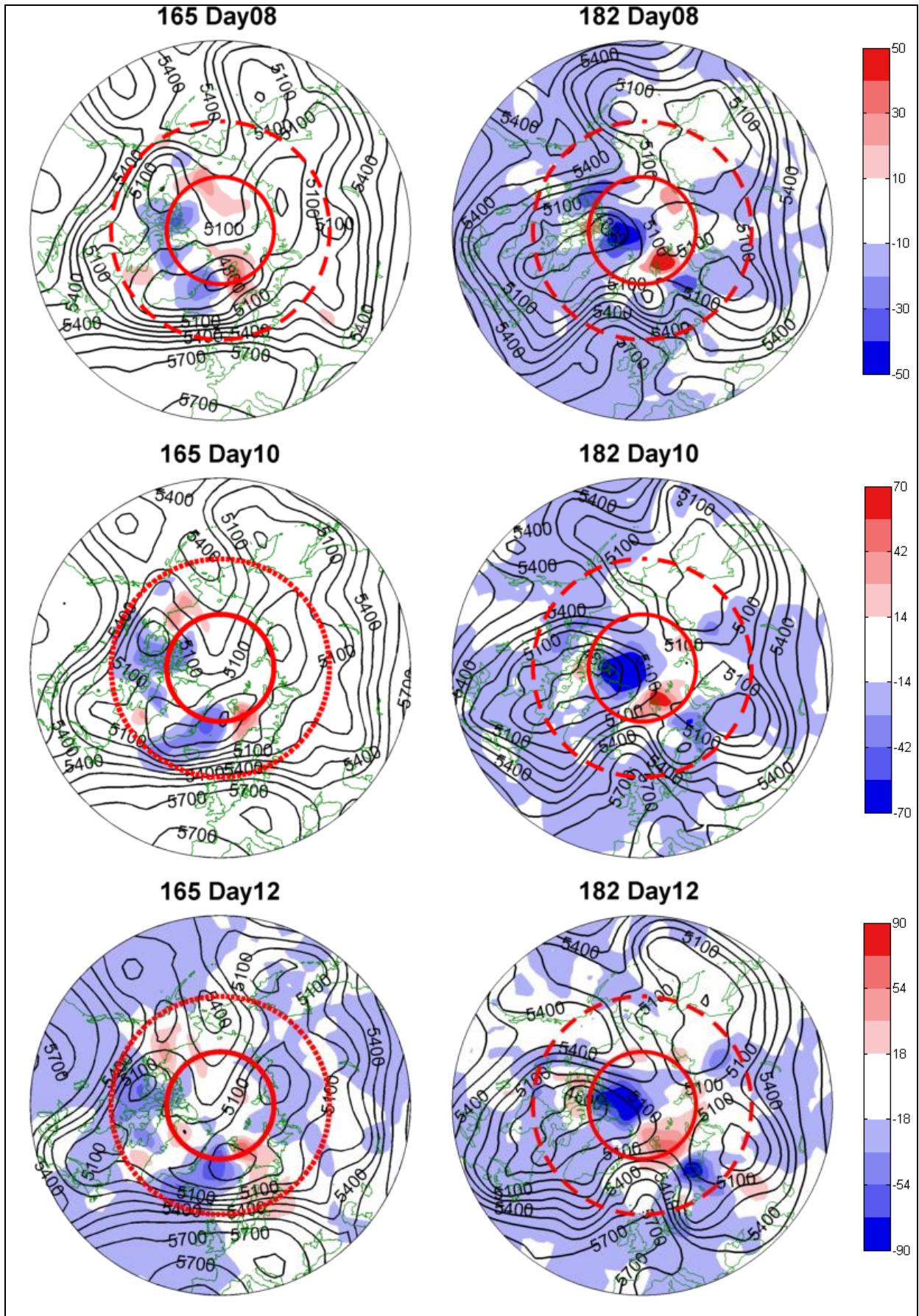
To illustrate the impact of relaxation on the weather forecast a several cases were studied in details. **Figure 23** shows the difference between the relaxed field and CNT for two forecast member that was strongly improved due to the relaxation. Note, that the scale is linearly increasing to capture the changes. Additionally the observed geopotential field is plotted with black curves. Two examples are shown. For the



forecast member no. 165 (started on 1<sup>st</sup> February 1993) the mean forecast error for Europe from day5 to day14 of the relaxed forecast was lower than that of CNT on 7 days (out of ten), the first four days were neglected as the effect of relaxation is small. For forecast member no.182 (forecast was started on 15<sup>th</sup> February 2001) the relaxed forecast was better than CNT on 8 days.

Small positive and negatives anomalies can be observed mainly in the relaxation region already at day 3. These anomalies grow with time and start to propagate towards south, eventually reaching northern Europe.







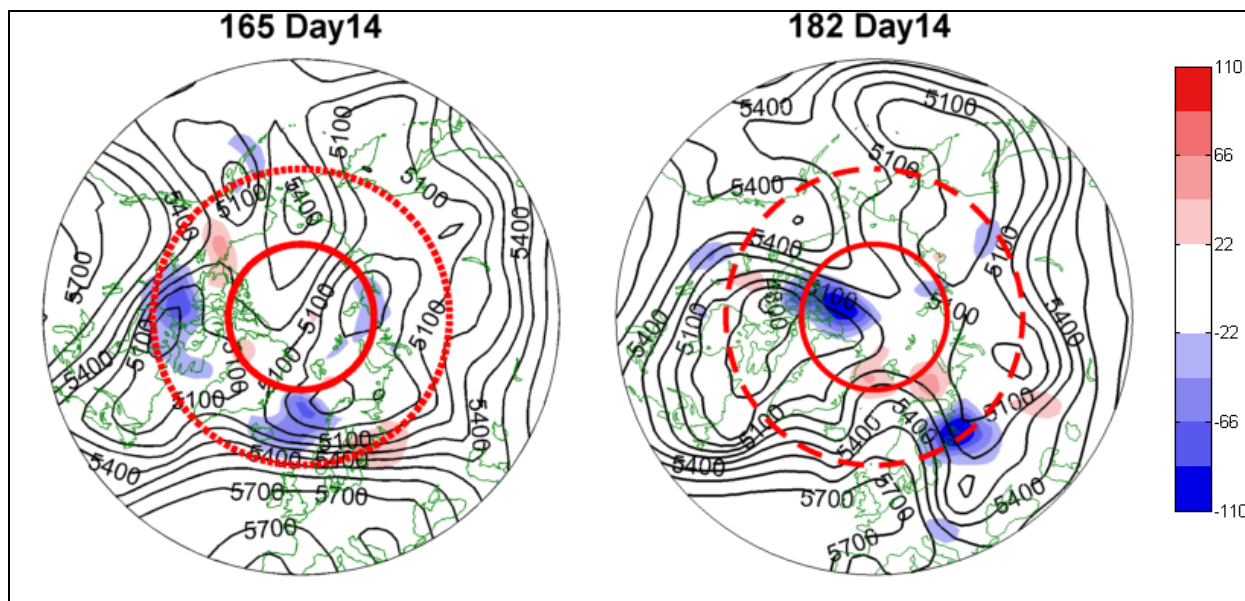


**Figure 23** The difference of the Z500 fields between relaxed field (R75) and CNT for two examples. Between day 5 and day 14 the error of the relaxed forecast was lower than the error of CNT on 7 days for forecast member no.165 and on 8 days for no. 182. The forecast member no.165 (left), started on 1st February 1993, no. 182 on 15th February 2001

#### 4.2.4 Trend analysis

As the time period investigated in this study (the last 34 years) is relatively long given the rapid changes going on in the Arctic, it was also investigated if a trend can be observed. For this purpose, the number of days for which the forecasts were improved due to the relaxation was averaged over each winter (6 forecast members for each winter). Furthermore, as the relaxation needs time to work, only day 5 to day 14 were considered. A negative trend could be observed only for winter months (**Figure 24**), indicating that during the last 34 years the effect of relaxation decreases with time. However, the variability between the years is large. Comparing the mean Z500 fields from years 1979-1995 and 1996-2012 shows that in the second half of the investigated period Z500 was higher over the Arctic and no west-east dipole structure, such as those shown in the composite plots can be observed. No trend was observed for other seasons.

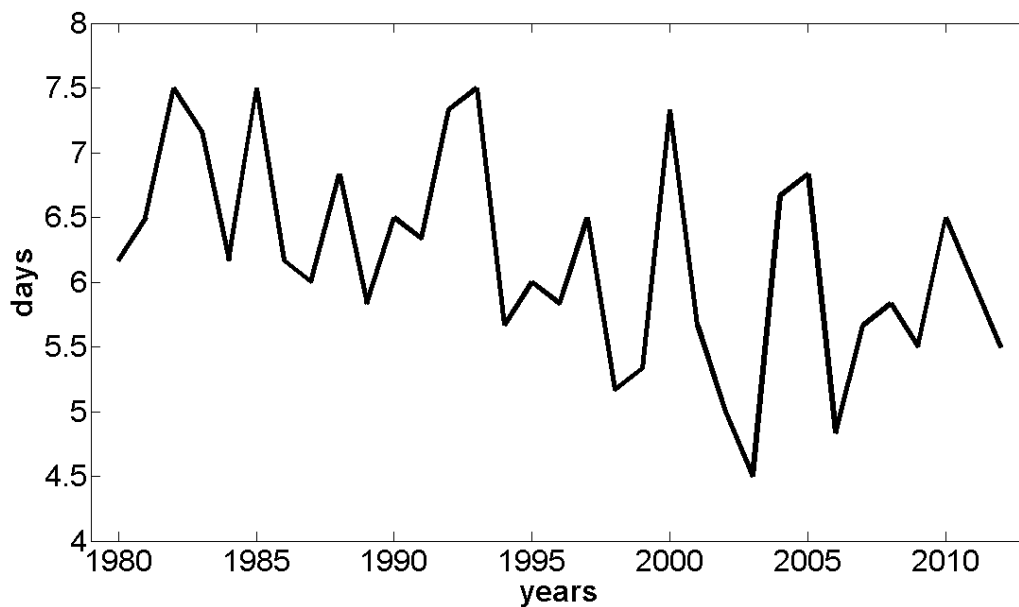


**Figure 24** Mean number of days that were improved due to the relaxation, averaged over winter (DJF). Only the period from day 5 to day 14 was considered, as within first 4 days the impact of relaxation is small.

## 5 Summary and discussion

The objective of this Thesis was to investigate the impact of the Arctic on the weather in Europe. A series of numerical experiments with artificially reduced forecast error in the Arctic applying a relaxation technique were performed using an operational weather forecast model from ECMWF.

First, winter-only data set of 88 monthly forecasts between 1980 and 2002 was analyzed (*Jung et al.2010a*). It was shown that “perfect knowledge” of the Arctic north of 70°N can reduce the forecast error for Europe as a region defined between 40°N-60°N and 20°W-40°E by 15% on average. However, if much smaller area north of 80°N (R80) is relaxed the error is reduced by approx. 5%.

Even more important is that the relaxation north of 70°N is much more affecting Europe than the relaxation in the tropics (between 20°N and 20°S). This may be surprising as the area of the relaxed region in the tropics is much larger. One reason is that Europe is closer to the Arctic than to the tropics and the signal thus needs less time to propagate. Moreover, the tropics are separated from Europe by the Subtropical High Belt that may prevent the signal from the tropic to propagate towards north. On the other hand, the relaxation region for R70 stretches into the region of polar jet stream. It is found where polar and sub-tropical air masses collide and therefore is a region that is synoptically very active. Since R80 is not providing such promising results as R70, it seems that the presence of polar jet stream could be of importance. However, the variation between individual forecast members is

high; in fact the standard deviation within the forecasts members is larger than the mean effect arising from the relaxation, suggesting that the signal to noise ratio is generally low.

It was also shown that when the forecast is improved due to the relaxation north of 70°N, in the first 15 days an anomalous air flow from the Arctic across Scandinavia can be observed bringing cold air into northern and eastern Europe. This is consistent with the result that in this region the error of the forecast is reduced up to 50% by relaxation. Furthermore the flow pattern resembles the negative phase of the NAO: the strength of the westerlies decreases and cold air from Siberia is transported into Europe. However, if the forecast error is calculated for the positive and negative phases of the NAO separately, it is not obvious what the dependency is as the differences between the different phases are very small. Moreover, the west-east dipole structure with anomalous high over Iceland and low over Barents Sea seems to be more crucial to explain the impact of the Arctic than the NAO pattern.

Furthermore it was examined if the results are sensitive to certain parameter choice of the analysis. Most of the analysis was based on 5-day means; but this time range was chosen rather arbitrarily to investigate the mean performance of the forecast and eliminate the synoptic variability (caused mainly by passage of low pressure systems). Repeating the analysis with 3-days mean does not change the conclusions: the mean effect of the relaxation has the same magnitude and structure, but daily variability are better captured. Also the results of the Z500 composite analysis are not very sensitive to the length of the averaging window, though the magnitude of the signal and its and statistical significance decrease.

In addition, it was tested whether the flow dependence of the mean impact changes if Europe is further divided into a western part (20W-20E: EUR-W) and an eastern part (20E-60E: EUR-E), as the impact of the relaxation was much higher in EUR-E with continental climate. For EUR-W, the anomalous northerly wind across Scandinavia (for whole Europe) changes to an anomalous north-easterly wind transporting cold air masses from northern Siberia. By contrast, in situations where the forecasts for EUR-E are improved an anomalous easterly wind that brings cold air masses from central Siberia is present. This shows that the results are very sensitive to the definition of Europe.



The message from the first set of experiments is that there are indications suggesting the impact of the Arctic on Europe. However the variability and randomness in the weather system is high, therefore the signal to noise ratio is low. Furthermore, the results are robust with respect to the choice of averaging length. Optimistic conclusion is that all methods applied to analyze the data coherently show that the Arctic has a non-negligible impact on European weather.

To improve the quality of the results in the second set of experiments the analysis was extended over all months between 1979 and 2012, providing 204 14-days forecast members for each season (winter, spring, summer and autumn). The temporal resolution was increased and averaging length of 24 hours was used, but the relaxation was applied to a smaller region north of 75°N. Comparing the effect of the relaxation in winter between the two sets of experiments, the error averaged over Europe within 14 days was reduced by approx.10% in first set and by 6% in the second set. This can be easily explained by the fact that the area north of 70°N is considerably larger. The length of the average window was also much longer in the first set of experiments (5 day versus 24h) so the small variations that increase the noise level could be better eliminated. Furthermore, the second set of experiment was run with a newer version of the model and with an improved data set (ERA Interim, instead of ERA-40). As the forecasting skill of the newer version of the model is higher, the relaxation can improve less.

Considering the differences between the seasons, it was shown that the mean forecast error for Europe is the highest in winter and the lowest in summer. The variability of the atmosphere is much higher in winter than in summer, as the temperature gradient between the Arctic and the tropics is stronger and consequently; the exchange of air masses enhanced. However, it does not mean that the quality of the summer forecast is higher, because the magnitude of anomalies in summer is lower.

There are also no large differences in the mean error reduction over Europe between the seasons. Only in summer the error reduction is slightly lower than in the other seasons, but the error itself is already smallest in summer so that the relaxation cannot lead to large improvements. Furthermore it was shown that the relaxation needs time: to work and it takes approx. 4 days for the signal to propagate into Europe.

The spatial structure of the error reduction over Europe shows different structures in different seasons. The error reduction in winter and spring is generally stronger for the whole of Europe. The effect of the relaxation occurs earlier (day6 for large parts of Europe), so the signal propagates faster in the colder seasons. In the first set of experiments the largest improvements were seen over northern and eastern Europe. The second set of experiments generally confirms this conclusion for winter, though, in south-eastern Europe the effect of the relaxation is reduced. Furthermore it was shown that in winter in the Atlantic region (especially the British Isles) forecast error was not notably reduced, suggesting that westerlies are stronger than the northerly wind. In other seasons the impact of the Arctic in that region seems to be comparable to the remainder of Europe.

The second set of experiments also shows that an anomalous southwards flow over Scandinavia is present when the forecast in Europe is improved. The magnitude is comparable to the first set of experiments, but the statistical significance is notably increased with the enlarged data set. Similar structures are present in spring (but weaker and shifted to the east) and autumn (still weaker and shifted to the west), but there are no meaningful flow dependencies in summer.

The second set of experiments confirmed the results from the first set of experiments. Additionally it was proved, that the impact of Arctic on Europe is strongest in winter and spring. Furthermore the outcome of the study shows that northern and eastern Europe and Siberia are important regions if the interactions between Polar Regions and mid-latitudes are concerned. This is consistent with other studies (Wu et al. 2011).

## 6 Conclusions and Outlook

The main conclusion from the study is that a better knowledge of the Arctic can indeed improve the skill of the weather forecast for Europe. However, the magnitude of the improvements strongly depends on the area of the relaxation, the time range of the forecast, and the season. The larger the area of the relaxation, the higher the impact. The longer the time range of the forecast, the more efficient the relaxation. Stronger improvements occur in cold seasons (winter and spring) than in the warm seasons. In winter the forecast error in Europe is reduced on average by 7% for in the first two weeks, and by 15% in the second half of the month. There are, however, large spatial differences, especially in winter. The highest improvement occurred in northern and eastern Europe. Here, the error of the forecast was reduced in winter by up to 50%. At the same time the forecast was not improved at all in the Atlantic region. The situation is different in other seasons where also in the Atlantic region forecasts were improved.

Furthermore it can also be concluded that the high impact of the Arctic, especially in winter in first 15 days of the forecast is stronger when an anomalous west-east dipole structure is present in Z500 field, with anomalous high over Iceland and anomalous low over Barents Sea. A resulting anomalous southwards air flow can be observed over Scandinavia. This anomalous flow, although weaker is also present in spring and autumn.

Another important conclusion is that improved knowledge of the Arctic will be especially beneficial for extended –range forecasts (beyond day 15), as on the one hand the existing forecasting systems are already performing well in the short and medium range, and on the other hand, the signal from the Arctic needs time to propagate south. However, for this time range, the flow dependence is not clear, as the signal to noise ratio was too low to make a meaningful statement.

It was also investigated how strong the impact of the Arctic is compared to the tropics. In winter, for most of Europe, the Arctic is more efficient in reducing the forecast error. Only in the Atlantic region and the Mediterranean region the tropics exert a stronger influence.

Although the results so far seem to be reasonable, the statistical significance is low because the variability of the data is large, both within a single forecast and between the forecasts. The atmosphere is strongly chaotic and thus a positive (negative)

impact of the relaxation on a forecast skill for a single forecast may well be by chance. However, even if the statistical significance is low, the results make sense from a physical point of view.

The outcome of the study may help in the further planning of forecasting systems. As with increased knowledge of the Arctic the forecast quality for Europe improves, it would be beneficial to have better observing systems in the Arctic. Furthermore this study provides evidence that further investigation of the processes in the Arctic, especially those considering sea ice, could help to guide future developments towards improved weather forecasts for Europe.

This study shows that the relaxation technique is a powerful tool to search for the origin of forecast errors, as well as to investigate remote impacts of certain regions.

Although consistent results have been provided so far, some questions remain open. The biggest problem is the high noise level. Therefore it would be beneficial to increase the sample size, especially in terms of number of forecasts. This way it may be possible to obtain more meaningful results concerning the flow dependence of the mean impact for the forecast range beyond day 15.

Another interesting question is if there are certain regions in the Arctic that are playing a special role in their relation to Europe, e.g. if the Atlantic region has stronger impact than the Pacific region. The composite analysis shows that especially the North Atlantic and the Barents Sea seem to be important. Such questions could be investigated further by applying the relaxation technique only to certain regions of special interest.

## 7 References

- Berry, Roger R., Chorley, R. J. 2010: *Atmosphere, Weather and Climate*, Ninth Edition, Routledge
- Dee, D. P., Uppala, S. M., Simmons, A. J. and co-authors, (2011), *The ERA-Interim reanalysis: configuration and performance of the data assimilation system*. Q.J.R. Meteorol. Soc., 137: 553–597. doi: 10.1002/qj.828
- Holton, James, 2004: *An introduction to dynamic meteorology*, Fourth Edition, Elsevier Academic Press, p.20 -21
- Jaiser, R.; Dethloff, K.; Handorf, D.; et al 2012: *Impact of sea ice cover changes on the Northern Hemisphere atmospheric winter circulation*, TELLUS SERIES A-DYNAMIC METEOROLOGY AND OCEANOGRAPHY, Volume:64, Article Number:11595
- Jung, Thomas, Miller, M.J., Palmer T.N., 2010a: *Diagnosing the Origin of Extended-Range Forecast Error*, Monthly Weather Review, **138**, 2434-2446
- Jung, Thomas, Palmer, T.N., Rodwell, M.J., Serrar, S., 2010b : *Understanding the anomalously cold European winter of 2005/06 using relaxation experiments*; Monthly Weather Review, **138**, 3157-3174
- Jung, Thomas, Vitart, F., Ferranti, L., Morcrette, J.-J., 2011, *Origin and predictability of extreme negative NAO winter of 2009/10*, Geophysical Research Letters, Vol. **38**, L07701, doi:10.1029/2011GL046786
- Kalnay, Eugenia 2003: *Atmospheric Modeling, data assimilation and predictability*, Cambridge University Press, p.141
- Klinker, E., 1990: *Investigation of systematic errors by relaxation experiments*. Quart. J. R. Meteorol. Soc., **116**, 573-594
- Lemke, P., Ren, J., Alley, R.B., Allison, I. and co-authors, 2007: *Observations: Changes in Snow, Ice and Frozen Ground*. In: *Climate Change 2007: The Physical Science Basis. Contribution of Working Group I to the Fourth Assessment Report of the Intergovernmental Panel on Climate Change* [Solomon, S., D. Qin, M. Manning, Z. Chen, M. Marquis, K.B. Averyt, M. Tignor and H.L. Miller (eds.)]. Cambridge University Press, Cambridge, United Kingdom and New York, NY, USA.

Lorenz, Edward, 1963, *Deterministic nonperiodic flow*, Journal of the Atmospheric Science, **20**, p.130-141

Lynch, Peter, 2007, *The origins of computer weather prediction and climate modeling*, Journal of Computational Physics, doi:10.1016/j.jcp.2007.02.034

Richardson, D.S., Bidlot, J., Ferranti, L., Ghelli, A., Gibert, C., Hewson, T., Janousek, M., Prates, F., Vitart, F., 2009, *Verification statistics and evaluations of ECMWF forecasts in 2008-2009*, ECMWF Technical Memorandum Nr. 606.

Semmler, Tido, McGrath, R., Wang, S., 2012, *The impact of Arctic sea ice on the Arctic energy budget and on the climate of the Northern mid-latitudes*, Springerlink.com, doi: 10.1007/s00382-012-1353-9

Simmons, A.J., Hollingsworth, A., 2001, Some aspects of the improvement of skill of numerical weather prediction, Quart. J. R. Meteorol. Soc., **128**, p.647-677

Uppala, S.M., Kållberg, P.W., Simmons, A.J. and co-authors, 2005: *The ERA-40 re-analysis*. Quart. J. R. Meteorol. Soc., **131**, 2961-3012. doi:10.1256/qj.04.176

Wallace, John, M., Hobbs, P.V. 2006: *Atmospheric Science: an Introductory Survey*, Second Edition, Elsevier

Wallace, John, M., Hobbs, P.V. 2006: *Atmospheric Science: an Introductory Survey*, Second Edition, Elsevier

Wu BingYi; Su J.Z., Zhang R.H., 2011: *Effects of autumn-winter Arctic sea ice on winter Siberian High*, CHINESE SCIENCE BULLETIN Volume: **56**, Issue 30, 3220-3228

# 8 Appendix

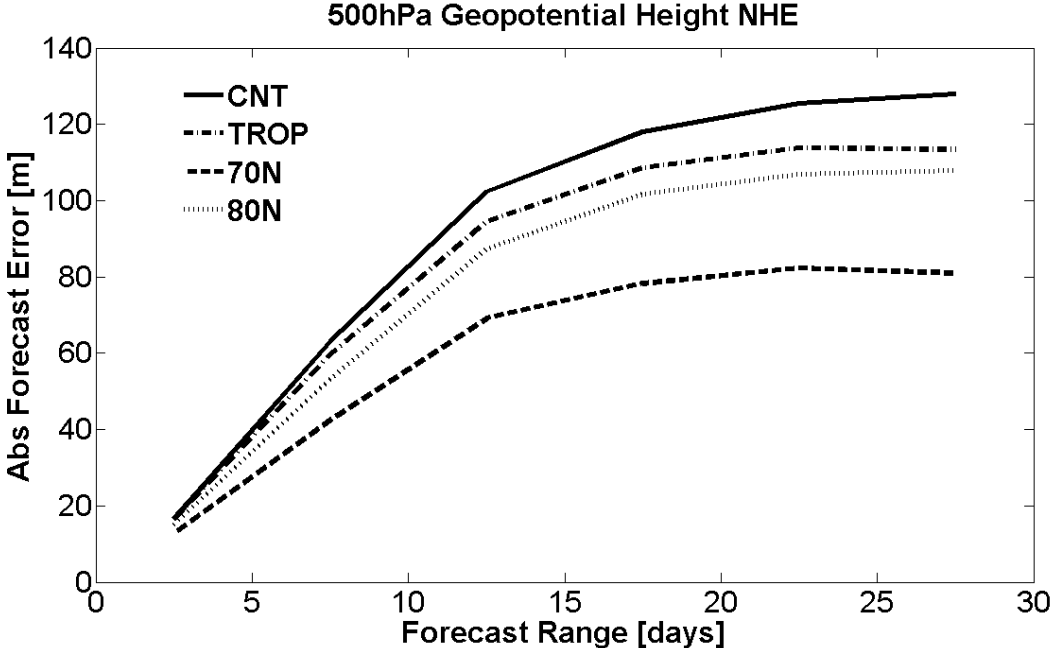


**Figure 25** Mean absolute error for 5-day-averaged forecasts of 500hPa geopotential height fields (m) over Northern Hemisphere Extratropics between 40°N-90°N for CNT (solid) as well as relaxed forecast, with relaxation region north of 70°N (R70, dashed), north of 80°N (R80, gray dotted) and in the Tropics (TROP, dash-dotted)

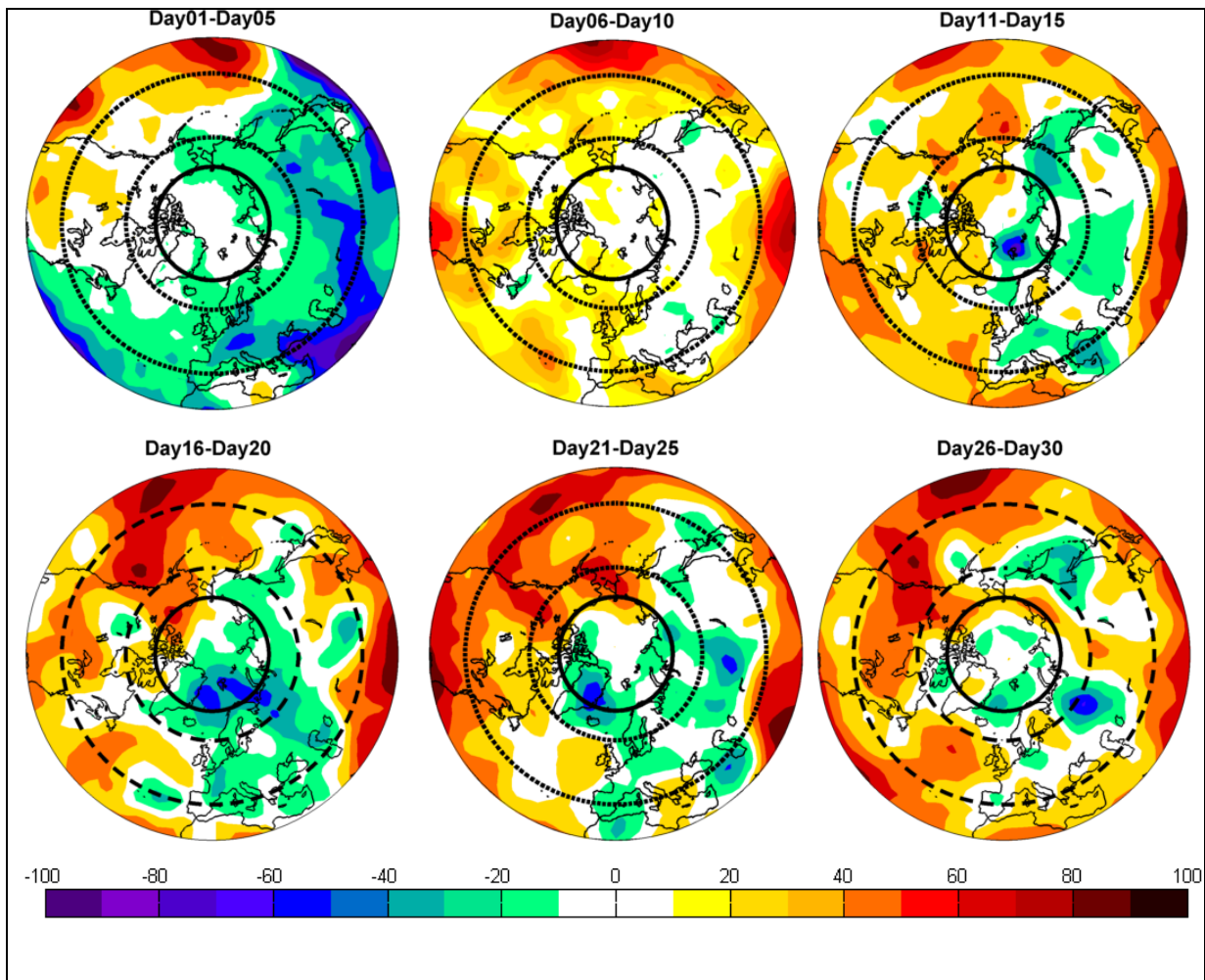


**Figure 26** Mean error reduction in % for winter-only experiment, for Northern Hemisphere Extratropics between 30°N -90°N after applying relaxation in the tropics (20°S-20°N). Black solid line indicates 70°N, the dashed line 60°N and 40°N.



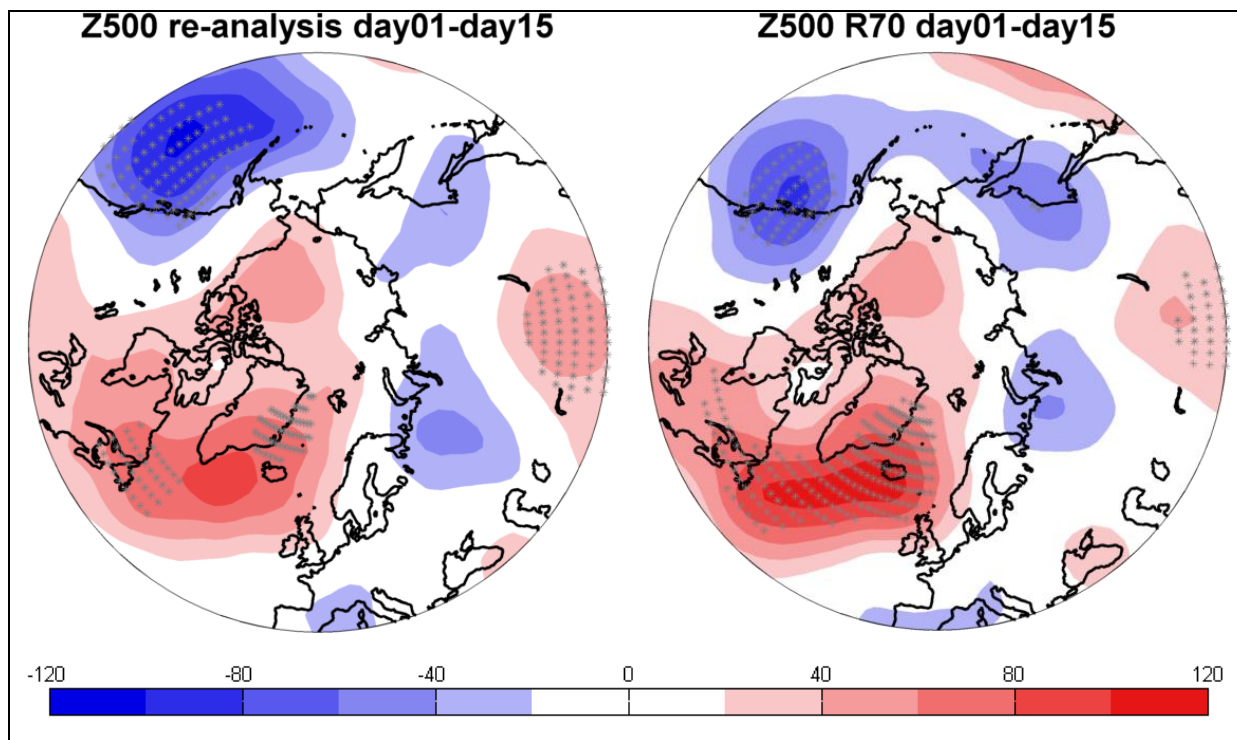


**Figure 27** Difference of the means of 500hPa geopotential height (m) between improved and worsened forecasts over Europe for day1-day15 in winter. Statistically significant grid points (Mann-Whitney ranksum test) are shown with gray stars. The 500hPa fields of the re-analysis are shown left; the simulated fields from forecast relaxed north of 70°N (R70) right.

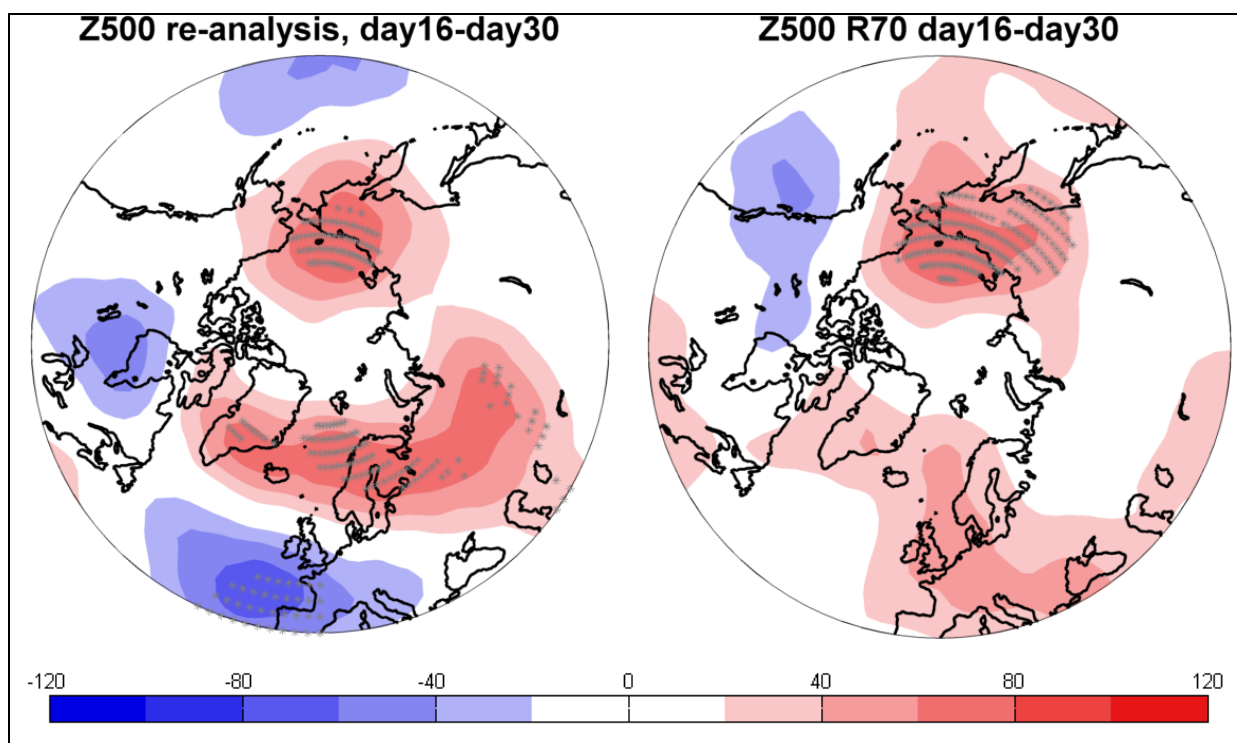


**Figure 28** Difference of the means of 500hPa geopotential height (m) between improved and worsened forecasts over Europe for day16-day30 in winter. Statistically significant grid points (Mann-Whitney ranksum test) are shown with gray stars. The 500hPa fields of the re-analysis are shown left; the simulated fields from forecast relaxed north of 70°N (R70) right.

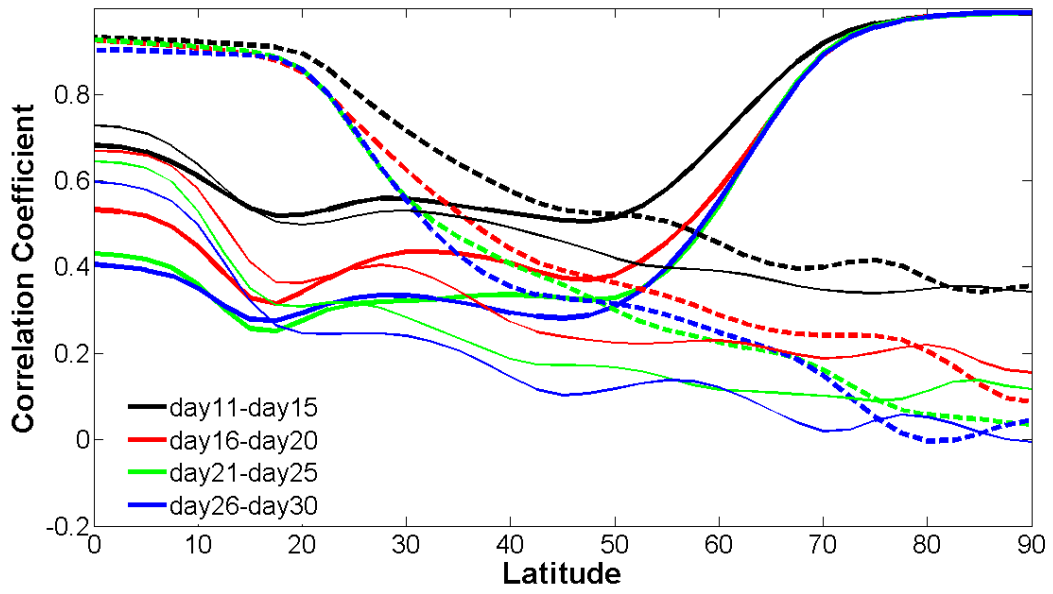


**Figure 29** Zonally averaged correlation coefficient between forecast and re-analysis for CNT (thin solid), forecast relaxed north of 70°N (thick solid) and forecast relaxed in the tropics between 20°S and 20°N (dashed).

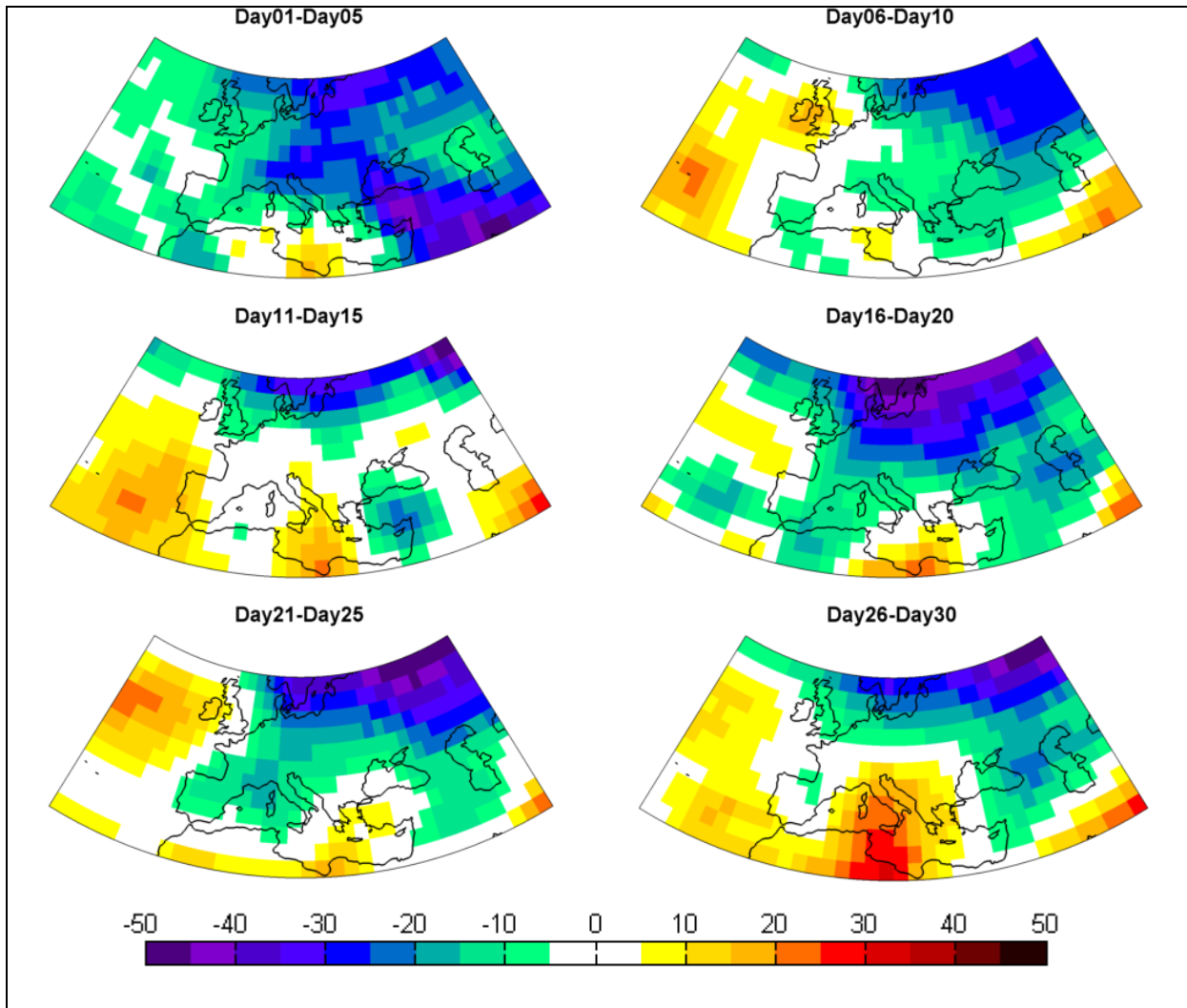


**Figure 30** The difference of the error reduction in % between the relaxation in the Tropics (20°S-20°N) and in the Arctic (70°N-90°N) shown for European region between 30°N-60°N and 30°W-60°E. The negative difference means that the relaxation in the Arctic is more effective in reducing the forecast error.

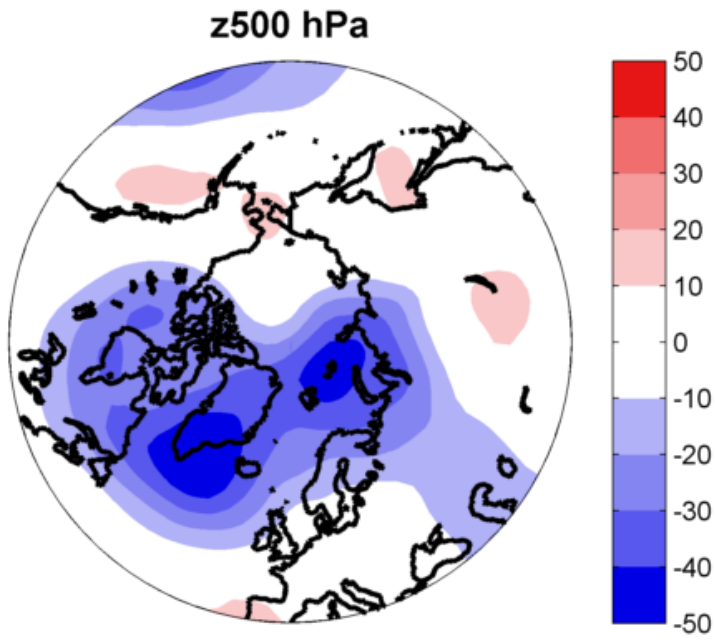


**Figure 31** The difference of the means between the years 1979-1995 and 1996-2012 of the 500hPa geopotential height (m) re-analysis in winter.

## 9 List of figures

Figure 1 An example of a 30-day forecast (black), relaxed forecast (dashed, red) and corresponding observations (blue). The parameter is the geopotential height at 500 hPa level, for the grid point 77.5°N and 45°E, the forecast started on 15 <sup>th</sup> February 1982.....	12
Figure 2 The difference between forecast error (averaged over Europe) between CNT and forecast relaxed above 70°N of all 88 forecast members. Mean value and the limit of one standard deviation are shown with blue curves. Two examples are highlighted with red curves. ....	18
Figure 3 It was looked for forecast members, for which the R70 was much better (“good”) or worse (“bad”) than CNT. Each time window was considered separately, to increase sample size, forecast members were grouped over larger time periods. The chart shows the sample sizes for the winter-only experiment, in dependence to chosen time period (day1-day15 or day16-day30) and time window chosen to average the data (3 or 5 days).....	20
Figure 4 The same as in Figure 3, but for the all-seasons experiment. ....	20
Figure 5 Mean absolute error for 5-day-averaged forecasts of 500hPa geopotential height fields (m) over Mid-latitudes between 40°N-60°N (left) and Europe between 40°N-60°N and 20°W-40°E (right) for CNT (solid) as well as relaxed forecast, with relaxation region north of 70°N (R70, dashed), north of 80°N (R80, gray dotted) and in the Tropics (TROP, dash-dotted).....	21
Figure 6 Mean reduction of the forecast error after applying relaxation technique north of 70°N (left) and north 80°N (right), averaged over Northern Hemisphere Extratropics 40°N-90°N (black), Mid-latitudes between 40°N and 60°N (magenta) and Europe between 40°N and 60°N as well as 20°W and 40°E. ....	22
Figure 7 Mean error reduction in % for winter-only experiment, for Northern Hemisphere Extratropics between 40°N -90°N after applying relaxation north of 70°N. Black solid line indicates the boundary of relaxation region (70°N), the dashed line 60°N. ....	23
Figure 8 Mean error reduction in % over European region between 40°N-60°N and 20°W-60°E for winter-only experiment for relaxation north of 70°N.....	24
Figure 9 Difference of the means of re-analysis fields (500hPa geopotential height in m) between improved and worsened forecasts over Europe for day1-day15 in winter.	

Statistically significant grid points (Mann-Whitney ranksum test) are shown with gray stars. The mean of improved and worsened forecasts was calculated of 5-day (left) or 3-day averaged (right) data. .... 26

Figure 10 Zonally averaged error reduction in % as a function of latitude between 30°N and 60° for the relaxation above 70°N(solid) and in the tropics (dashed) between 20°S and 20°N. .... 27

Figure 11 The difference of zonally averaged correlation coefficient between forecast relaxed north of 70°N and CNT (solid) as well as between forecast relaxed in the tropics between 20°S and 20°N and CNT (dashed). The correlation coefficient was calculated for each grid point between the forecast and the re-analysis. .... 28

Figure 12 The difference of the error reduction in % between the relaxation in the tropics (20°S-20°N) and in the Arctic (70°N-90°N). The negative difference means that the relaxation in the Arctic is more effective in reducing the forecast error. The solid line indicate the 70°N, the dashed lines indicate boundaries of mid-latitudes (40°N-60°N). .... 31

Figure 13 Mean error reduction in % over European region between 40°N-60°N and 20°W-60°E for winter-only experiment, calculated as 3-day average. .... 32

Figure 14 Mean absolute error of 5-day-averaged forecasts of 500hPa geopotential height fields (m) over whole Europe between 40°N-60°N and 20°W-40°E (black) as well as maritime, western Europe between 20°W and 20°E(red) and continental, eastern Europe between 20°E and 60°E (green); for CNT (solid) as well as relaxed forecast, with relaxation region above 70°N (R70, dashed) and in the Tropics (TROP, dash-dotted). .... 34

Figure 15 Difference of the means of re-analysis fields (500hPa geopotential height in m) for day1-day15 in winter between improved and worsened forecasts for western Europe (20°W-20°E, left) and eastern Europe (20°E-60°E, right). Statistically significant grid points (Mann-Whitney ranksum test) are shown with gray stars. .... 35

Figure 16 Mean absolute error of 1-day-averaged forecasts of 500hPa geopotential height fields (m) over Europe for CNT (solid) and forecast relaxed over 75°N (dashed) for winter (black), spring (green),summer (red) and autumn(blue). .... 36

Figure 17 Mean error reduction after applying relaxation north of 75°N, averaged over Northern Hemisphere Extratropics (40°N-90°N, black), Mid-latitudes (40°N-60°N, magenta) and Europe (40°N-60°N and 20°W-40°E, green), for winter (solid, thick), spring (solid, thin), summer (dotted) and autumn (dashed). .... 37

Figure 18 Mean error reduction in % over European region between 40°N-60°N and 20°W-60°E for winter (DJF). .....	38
Figure 19 Mean error reduction in % over European region between 40°N-60°N and 20°W-60°E for spring (MAM). .....	39
Figure 20 Mean error reduction in % over European region between 40°N-60°N and 20°W-60°E for summer (JJA). .....	40
Figure 21 Mean error reduction in % over European region between 40°N-60°N and 20°W-60°E for autumn (SON). .....	41
Figure 22 Difference of the means of re-analysis fields (500hPa geopotential height in m) between improved and worsened forecasts over Europe for day1-day14. Statistically significant grid points (Mann-Whitney ranksum test) are shown with gray stars. data.....	42
Figure 23 The difference of the Z500 fields between relaxed field (R75) and CNT for two examples. Between day 5 and day 14 the error of the relaxed forecast was lower than the error of CNT on 7 days for forecast member no.165 and on 8 days for no. 182. The forecast member no.165 (left), started on 1st February 1993, no. 182 on 15th February 2001 .....	46
Figure 24 Mean number of days that were improved due to the relaxation, averaged over winter (DJF). Only the period from day 5 to day 14 was considered, as within first 4 days the impact of relaxation is small. ....	47
Figure 25 Mean absolute error for 5-day-averaged forecasts of 500hPa geopotential height fields (m) over Northern Hemisphere Extratropics between 40°N-90°N for CNT (solid) as well as relaxed forecast, with relaxation region north of 70°N (R70, dashed), north of 80°N (R80, gray dotted) and in the Tropics (TROP, dash-dotted)	55
Figure 26 Mean error reduction in % for winter-only experiment, for Northern Hemisphere Extratropics between 30°N -90°N after applying relaxation in the tropics (20°S-20°N). Black solid line indicates 70°N, the dashed line 60°N and 40°N. ....	56
Figure 27 Difference of the means of 500hPa geopotential height (m) between improved and worsened forecasts over Europe for day1-day15 in winter. Statistically significant grid points (Mann-Whitney ranksum test) are shown with gray stars. The 500hPa fields of the re-analysis are shown left; the simulated fields from forecast relaxed north of 70°N (R70) right.....	57
Figure 28 Difference of the means of 500hPa geopotential height (m) between improved and worsened forecasts over Europe for day16-day30 in winter. Statistically	

significant grid points (Mann-Whitney ranksum test) are shown with gray stars. The 500hPa fields of the re-analysis are shown left; the simulated fields from forecast relaxed north of 70°N (R70) right. .... 57

Figure 29 Zonally averaged correlation coefficient between forecast and re-analysis for CNT (thin solid), forecast relaxed north of 70°N (thick solid) and forecast relaxed in the tropics between 20°S and 20°N (dashed). .... 58

Figure 30 The difference of the error reduction in % between the relaxation in the Tropics (20°S-20°N) and in the Arctic (70°N-90°N) shown for European region between 30°N-60°N and 30°W-60°E. The negative difference means that the relaxation in the Arctic is more effective in reducing the forecast error. .... 59

Figure 31 The difference of the means between the years 1979-1995 and 1996-2012 of the 500hPa geopotential height (m) re-analysis in winter. .... 60